MHD-NATURAL CONVECTION IN POROUS MEDIA-FILLED ENCLOSURES

By
Fadi Ghassan Shehadeh

Supervisor
Dr. Hamzeh M. Duwairi

This Thesis was Submitted in Partial Fulfillment of the Requirements for the Master's Degree of Science in Mechanical Engineering

Faculty of Graduate Studies
The University of Jordan

November, 2008

ii

COMMETEE DECISION

This Thesis/Dissertation (MHD-NATURAL CONVECTION IN POROUS MEDIA-FILLED ENCLOSURES) was successfully defended and approved on November 27-2008.

Examination Committee	Signature
Dr. Hamzeh Duwairi (Supervisor) Association Prof of thermal	
Dr. Ahmad Al-Salaymeh (Member) Association Prof of thermal	
Dr. Jehad Yamin (Member) Assistant Prof of combustion	
Dr. N.Beithou (Member) Association Prof of thermal (Applied Science University)	

DEDICATION

- *To my father, who has given his unlimited and unconditional love and care, without his support, I could not succeed.*

- *To my loving mother, whose presence has been my motivation.*

- *To my brothers and sister: Ali, Mohammad, Dena, Fesal, Anas.*

- *To all whom I love.*

ACNOWLEDGMENT

We would like to express our deepest regards to Dr. Hamzeh M.Duwairi for his help and advice throughout this work. We also would like to thanks extended to the committee. Finally, we thank all those people who provided us with information, help, advice and support. And for all, we dedicate this project.

LIST OF CONTENTS :

FIGURE	Description
3.1	Schematic of physical model and coordinate system
4.1	Nodal points used.
4.2	Typical dimensionless streamline and dimensionless temperature patterns
4.3	Variation of mean Nusselt number with Ra_w for various A.
5.1	Typical dimensionless streamline and dimensionless temperature patterns for various magnetic influence number (a) $Ha^2 = 0$, (b) $Ha^2 = 0.03$, (c) $Ha^2 = 0.1$, (d) $Ha^2 = 1$, (e) $Ha^2 = 3$, (f) $Ha^2 = 4$ for ϕ=30°, A = 1, Fr = 0.01, and Ra_w = 100
5.2	Variation of Nu-mean with Ha^2 for an enclosure
5.3	Typical dimensionless streamline and dimensionless temperature patterns for various Darcy-modified Rayleigh number (a) $Ra_w = 1$, (b) $Ra_w = 50$, (c) $Ra_w = 100$, for ϕ=30°, A = 1, Fr = 0.01, and $Ha^2 = 0.02$
5.4	Variation of Nu-mean with Raw for an enclosure for various A for Ø=30°, Fr = 0.01, and $Ha^2 = 0.02$
5.5	Typical dimensionless streamline and dimensionless temperature patterns for various inclination angle of the enclosure (a) $\phi = 0$, (b) $\phi = 90°$ for $Ra_w = 100$, A = 1, Fr = 0.01, and $Ha^2 = 0.02$
5.6	Variation of mean Nusselt number and dimensionless center-stream function with angle of inclination for an enclosure for various Ha^2 for $Ra_w = 100$, A = 1, Fr = 0.01
5.7	Variation of mean Nusselt number and dimensionless center-stream function with angle of inclination for an enclosure for various Ra_w for A = 1, Fr = 0.01,

Nomenclature

A	The aspect ratio of the enclosure.
$\vec{B}$	The magnetic field strength vector, [wb/ m^2]
B_0	magnatic field strength, [wb/ m^2]
C_F	Forchheimer constant.
c_p	Specific heat at constant pressure, [kJ/kg.K]
d	Diameter of spherical beads.[m]
$\vec{E}$	The electric field vector, [volt/ m]
$\vec{F}_e$	The magnetic force, [N]
$\vec{F}_{em}$	The total electromagnetic force, [N]
$\vec{F}_m$	The total electromagnetic force, [N]
Fr	Forchheimer number.
g	Gravitational acceleration, [m/ s^2]
Ge	The Gebhart number.
H	The length in y-direction, [m]
$\vec{H}$	The magnetic field intensity. [ampere/ m]
Ha^2	The magnetic influence number.
$\vec{J}$	The current density, [ampere/ area]
$\vec{J}_c$	The conduction current flow.
$\vec{J}_{md}$	The magnetic field induces a current in the conductor.
K	Permeability, [m^2]
k	Thermal conductivity of the porous media and fluid, [W/m.K]
P	Pressure, [Pa]
Ra_w	Modified Rayleigh number.

T Temperature, [K]

T_c The cold wall temperature, [K]

T_H The hot wall temperature, [K]

T_0 The reference temperature, [K]

u The velocity in x direction, [m/ s]

$\vec{V}$ The velocity of the conductor, [m/ s]

v The velocity in y direction, [m/ s]

W_{em} The work done on the system per unit time by the electromagnetic force, [Watt]

W The length in x-direction, [m]

Greek symbols

α_a Thermal diffusivity, $[m^2/ s]$

μ Absolute viscosity, [kg/m.s]

μ_0 The magnetic permeability.

ν Dynamic viscosity, $[m^2/ s]$

ε Porosity.

ρ The fluid density, $[kg/ m^3]$

ρ_0 The fluid density at some reference temperature, $[kg/ m^3]$

ρ_e The charge density.

σ Electrical conductivity, $[m\Omega/m^2]$

β Coefficient of thermal expansion, $[K^{-1}]$

Ø The inclination angle of the enclosure, [degrees]

ψ Streamline function.

Ψ Dimensionless stream function.

Subscripts

i To describe the nodal points in the x-direction.

j To describe the nodal points in the y-direction.

N Number of nodal points in the y-direction.

M Number of nodal points in the x-direction.

Δx The increment in the x-direction.

Δy The increment in the y-direction.

centre The centre of the enclosure.

Mean The average Nusselt number.

MHD-NATURAL CONVECTION IN POROUS MEDIA-FILLED ENCLOSURES

By
Fadi Ghassan Shehadeh

Supervisor
Dr. Hamzeh M. Duwairi

Abstract

In this work the magnetohydrodynamics natural convection heat transfer with Joule and viscous heating effects inside a porous media filled inclined rectangular enclosures has been investigated numerically. The boundary conditions selected on the enclosure are two adiabatic and two isothermal walls. The governing equations, continuity, Forchheimer extension of Darcy law and energy, are going to be transformed into dimensionless form using a set of suitable variables then solved numerically using a finite difference scheme. The governing parameters are magnetic effect, Gebhart number, Modified Rayleigh number, inclination angle, and the aspect ratio of the enclosure. It is found that the heat transfer and fluid flow are decreased with the increasing of magnetic influence number, but they are increased with the increasing of Modified Rayleigh number and the Aspect ratio. By increasing Gebhart number the heat transfer and fluid flow inside the enclosure are increased.

Chapter 1

Introduction

1.1 Introduction:

It is very important to get better understanding of the flow in a porous media. Many processes in nature involve transport processes in such media. In many parts of the world water that has been stored for thousands of years in large volumes of porous rock is an important asset. Similarly the world supply of oil was formed and stored under special circumstances in porous rock formations. Other processes, which involve flow in a porous media, are frost heaves, filtration or straining and sewage purification in sand beds. The flow of homogeneous fluids through porous media is sufficiently wide in scope to find applications in many branches of applied science. By the term homogeneous fluid is meant essentially a single-phase fluid. This may be either a gas or a liquid.

The study of fluid, which is electrically conducted and moves in a magnetic field, is known as a magneto hydrodynamics (MHD), it is a relatively new but important branch of fluid dynamics, when a conducting fluid such as mercury moves through a magnetic field, the generated current interacts with the magnetic field to produce a body force on the fluid. The study of MHD flow in a porous media becomes very important in nuclear reactors, where the MHD effect is very dangerous and important.

The general nature of the porous media:

1- Porosity, which is a measure of the pore space and hence of the fluid capacity of the medium.

2- Permeability, which is a measure of the ease with which fluids may transfer through medium under the influence of a driving pressure.

1.2 Darcy's Law:

Henry Darcy's (1856) investigations into the hydrology of the water supply of Dijon and his experiments on steady-state unidirectional flow in a uniform medium revealed proportionality between flow rate and the applied pressure difference. In modern notation this is expressed, in refined form, by

$$u = -\frac{K}{\mu}\frac{\partial P}{\partial x} \tag{1.1}$$

Here $\partial P/\partial x$ is the pressure gradient in the flow direction and μ is the dynamic viscosity of the fluid. The coefficient K is independent of the nature of the fluid but it depends on the geometry of the medium and it is known as the permeability.

1.3 Forchheimer's Equation:

Darcy's equation (1.1) is linear in the velocity u, it holds when u is sufficiently small. In practice, "sufficiently small" means that the Reynolds number Re of the flow, based on a typical pore or particle diameter, is of order unity or smaller. As u increases, the transition to nonlinear drag is quite smooth; there is no sudden transition as Re is increased in the range 1 to 10. Clearly this transition is not one from laminar to turbulent flow, since at such comparatively small Reynolds numbers the flow in the pores is still laminar. Rather, the breakdown in linearity is due to the fact that the form drag due to solid obstacles is now comparable with the surface drag due to friction. The appropriate modification to Darcy's equation is to replace Eq. (1.1) by

$$u = -\frac{K}{\mu}\frac{\partial P}{\partial x} + \frac{C_F \rho}{\sqrt{K}}u^2 \tag{1.2}$$

where C_F is a dimensionless form-drag constant. Equation (1.2) is a modification of an equation associated with the names of Dupuit (1863) and Forchheimer (1901). The geometric function C_F (Forcheimer number) and the permeability of the porous medium K are based on Ergun's empirical expression, Ergun (1952), which may be used for the packed beds that may be closely modeled as spherical beads of diameter, d, and is given by

$$K = \frac{\varepsilon^3 d^2}{150(1-\varepsilon)^2} \tag{1.3}$$

$$C_F = \frac{1.75}{(150\varepsilon^3)^{1/2}} \tag{1.4}$$

where (d) is the particle pure diameter, and (ε) is the porosity.

1.4 Oberbeck-Boussinesq Approximation:

In studies of natural convection we add the gravitational term ρg to the right-hand side of the Forchheimer's equation (1.2) or its appropriate extension. For thermal convection to occur, the density of the fluid must be a function of the temperature, and hence we need an equation of state to complement the equations of mass, momentum, and energy. The simplest equation of state is

$$\rho = \rho_0\big(1 + \beta(T - T_0)\big) \tag{1.5}$$

where ρ_0 is the fluid density at some reference temperature T_0 and β is the coefficient of thermal expansion. In order to simplify the subsequent analysis, one employs the Boussinesq approximation whenever it is valid. Strictly speaking, one should call this the Oberbeck-Boussinesq approximation, since Oberbeck (1879) has priority over Boussinesq (1903), as

documented by Joseph (1976). The approximation consists of setting constants all the properties of the medium, except that the vital buoyancy term involving β is retained in the momentum equation.

1.5 Heat transfer in magneto hydrodynamic (MHD) system:

Magneto hydrodynamics (MHD) is a relatively new but important branch of fluid dynamics. It is concerned with the interaction of electrically conducting and electromagnetic fluids. When a conducting fluid moves through a magnetic field, an electric field and consequently a current may be induced and, in turn, the current interacts with the magnetic field to produce a body force on the fluid. MHD flow occurs in the sun, the earth's interior, the ionosphere, and the stars and their atmosphere, and many new devices have been made which utilize the fluid electromagnetic field interactions, such as travelling wave tubes, electrical discharges, and many others. Some basic electromagnetic concept as follows:

For a neutrally charged system the current density $\vec{J}$ is given by:

$$\vec{J} = \sigma . \vec{E} \tag{1.6}$$

Where σ is the electrical conductive and $\vec{E}$ is the electric field vector. The magnetic field strength $\vec{B}$ is expressed by:

$$\vec{B} = \mu_0 . \vec{H} \tag{1.7}$$

Where μ_0 is called the magnetic permeability and $\vec{H}$ is the Magnetic field intensity. The force exerted on a system of charged particles by an electric field is given by:

$$\vec{F}_e = \rho_e . \vec{E} \tag{1.8}$$

Where ρ_e is the charge density. The magnetic force exerted on a current carrying conduction is expressed by:

$$\vec{F}_m = \vec{J} \times \vec{B} \tag{1.9}$$

The total electromagnetic force is given by:

$$\vec{F}_{em} = \rho_e . \vec{E} + \vec{J} \times \vec{B} \tag{1.10}$$

The work done on the system per unit time by the electromagnetic force is expressed by:

$$W_{em} = \vec{F}_{em} . \vec{V} \tag{1.11}$$

Where V is the velocity of the conductor.

The magnetic field induces a current in the conductor is given by:

$$\vec{J}_{md} = \sigma(\vec{V} \times \vec{B}) \tag{1.12}$$

Then, the conduction current flow is given by:

$$\vec{J}_c = \sigma(\vec{E} + \vec{V} \times \vec{B}) \tag{1.13}$$

And the total current flow is given by:

$$\vec{J} = \vec{J}_c + \rho_e . \vec{V} \tag{1.14}$$

For the electromagnetic work Holman (1990):

$$W_{em} = \vec{E} . \vec{J} - \frac{\vec{J}_c . \vec{J}_c}{\sigma} \tag{1.15}$$

The fluid dynamical aspects of MHD are handled by adding the electromagnetic force and work to non-Darcy equations and energy equation respectively. The governing equations that describe the problem under consideration can be written as: The continuity equation:

$$\frac{\partial u}{\partial x} + \frac{\partial v}{\partial y} = 0 \tag{1.16}$$

The momentum equation in x and y-directions:

$$\frac{\mu u}{K} + \frac{\rho C_F}{\sqrt{K}} u^2 + \sigma B_0^2 u = -\frac{\partial P}{\partial x} + \rho \beta g (T - T_c) \cos\emptyset \tag{1.17}$$

$$\frac{\mu v}{K} + \frac{\rho C_F}{\sqrt{K}} v^2 + \sigma B_0^2 v = -\frac{\partial P}{\partial y} + \rho \beta g (T - T_c) \sin\emptyset \qquad (1.18)$$

The energy equation:

$$u\frac{\partial T}{\partial x} + v\frac{\partial T}{\partial y} = \frac{k}{\rho c_p}\left(\frac{\partial^2 T}{\partial x^2} + \frac{\partial^2 T}{\partial y^2}\right) + \frac{\nu}{K c_p} u \left(u + \frac{C_F \sqrt{K}}{\nu} u^2\right) + \frac{\sigma B_0^2}{\rho c_p} u^2 \qquad (1.19)$$

Where the term (σB_0^2) represents the effect of magnetic field force on the fluid velocity, and the term $(\frac{\sigma B_0^2}{\rho c_p})$ represents the work done by magnetic field force on the fluid.

Chapter 2

Literature Review

Since the early work of Darcy in the 19th century, extensive investigations have been conducted on flow and heat transfer through porous media, covering range of different fields and application such as geothermal operation, nuclear reactors, transpiration cooling, and building thermal insulation.

Magneto hydrodynamics has been a subject for many researchers in the field. Henoch and Meng (1991) used the magnetic force to retard the transition to the turbulent boundary layer and reduce the frictional Darcy force. Kim and Lee (2000) set up an experiment using a circular cylinder where electrodes and magnets are installed in an alternative sequence in axial direction of the cylinder to generate magnetic force in the circumferential direction. Many authors had studied the effects of magnetic on mixed, natural and forced convection heat transfer problems. Chandra and Gosh (2001) studied the effect of magnetic field on electrically conducted visco-elastic fluid; they found in such a flow that the velocity field decreases with increase of magnetic field strength. Sparrow and Cess (1961) investigated the free convection heat transfer due to the simultaneous action of buoyancy and induced magnetic forces; the analysis is carried out for laminar boundary-layer flow about an isothermal vertical plate. They found that the free convection heat transfer to liquid metals may be significantly affected by the presence of magnetic field, but that very small effects are experienced by other fluid. Raptis and Singh (1983) studied the effect of a uniform transform transverse magnetic field on the free convection flow of an electrically conducting fluid past an infinite vertical plate for classes of impulsive as well as uniformly accelerated motion of the plate. They found that the effect of the magnetic field is to increase the velocity field on both cases.

Jha (2001) discussed the combined effect of natural convection and uniform transverse magnetic field on the Couette flow of an electrically conducting fluid between two parallel plates for impulsive motion of one plate. Comparative study is made between rile velocity field for magnetic field fixed with respect to plate and a fixed magnetic field with respect to the fluid. Hossain (1992) had studied the effect of viscous and Joule heating on the flow of an electrically conducting and viscous incompressible fluid past a semi-infinite plate of which temperature varies linearly with the distance from the leading edge and in the presence of uniform transverse magnetic field. The equations governing the flow are solved numerically applying the finite difference method along with Newton's linearization approximation. The combined effects of forced and natural convection heat transfer in the presence of transverse magnetic field from vertical surfaces are studied by many researchers. Garandet et al. (1992) had analyzed the equations of the magneto hydrodynamics that can be used to model the effect of a transverse magnetic field on the buoyancy driven convection in a two dimensional cavity.

Aldoss et al.(1995) Studied the effect of mixed convection heat transfer from a vertical plate embedded in a saturated porous medium and subjected to a uniform magnetic field. They found the strength of the magnetic field has an effect on the Nusselt number and wall shear stress and the increasing of the magnetic field strength has the effect of decreasing the local Nusselt number in the mixed convection regime.

Recently, Duwairi and Damseh (2004, a) studied the effects of MHD-natural convection heat transfer from radiating vertical porous surfaces, they found non-similarity parameter to solve this problem with fluid suction or injection along the stream wise coordinate and found that the increasing of the magnetic field strength decreases the velocity and the heat transfer rates inside

the boundary layer. Duwairi and Duwairi (2004, b) studied the thermal radiation heat transfer effects on the MHD-Rayleigh flow of gray viscous fluids under the effect of a transverse magnetic field, the free convection heat transfer problem from constant surface heat flux moving plate is selected for study. They found that the increasing of the magnetic field strength decreased the velocity inside the boundary layer. Duwairi and Al-Araj (2004, c) studied the MHD-thermal radiation interaction along a vertical cylinder embedded in a plain medium; they found that the increasing of magnetic forces decreased velocities and heat transfer rates to the conductive fluids. Duwairi and Al-Kablawi (2006) formulated the MHD-conjugative heat transfer problem from vertical surfaces embedded in saturated porous media; the inclusion of conduction parameter to the MHD traditional mixed convection problem is achieved. Duwairi et al. (2006) studied the transient MHD natural convection heat transfer problem using non-Boussinesq approximation. Hammad and Duwairi (2008) solved the non-Newtonian MHD convection heat transfer problem a round a non isothermal cylinder and spheres. A gain the magnetic forces had a retarding effects on the flow and heating effect of the fluid layers, which had decreased the local Nusselt numbers.

In all the previous studied the MHD effects for externally flow are investigated either for fluid flow in a plain or a porous media, but little attention is given to the internal flow heat transfer problem due to complexity in solving for the pressure gradients inside different conduits. In this study the MHD-natural convection interaction inside rectangular porous filled enclosures are going to be formulated using continuity, Forchheimar of Darcy law and energy, the governing equations are going to be transformed into dimensionless form using a set of suitable variables then solved. Two sides of the rectangular enclosure are adiabatic and the other two are isothermal. Different streamline profiles, dimensionless temperature profiles and local Nusselt

numbers are going to be drawn. Comparison with previous works available in limits of a traditional non conductive fluid is going to be laid. The parameters that describe the problem under consideration are; inclination angle parameter, aspect ratio parameter, magnetic effect parameter, Joule and viscous heating effects parameters of the rectangular porous media-filled enclosure, and the modified Rayleigh number.

Chapter 3

Problem Formulations

3.1 Introduction:

Several analytical studies have been performed in recent years relating to the problem of steady two-dimensional heat transfer by natural convection across porous media-filled rectangular enclosures which is, in general, inclined at an angle. In this work the magneto hydrodynamics natural convection heat transfer problem inside a porous media filled inclined rectangular enclosures is going to be studied. One wall of the enclosure is kept at uniform high temperature and the opposite is kept at a uniform low temperature. The other two walls of the enclosure are adiabatic, i.e., it is assumed that no heat is transferred into or out of walls.

3.2 Analysis:

In this study, the geometry considered is inclined rectangular enclosure, which embedded in a fluid-saturated porous media as shown in figure (3.1). The following important assumptions are made in order to obtain the governing equations:

1. The flow is steady and two dimensional.
2. The thermo physical properties of the fluid are homogeneous and isotropic.
3. The temperature of the fluid is everywhere below the boiling point.
4. The magnetic field is uniform throughout the boundary layer.
5. The fluid inside the enclosure is incompressible fluid.

Under these assumptions the governing equations which describe the problem are:

The continuity equation:

$$\frac{\partial \mathrm{u}}{\partial \mathrm{x}} + \frac{\partial \mathrm{v}}{\partial \mathrm{y}} = 0 \qquad (3.1)$$

The momentum equation in x and y-directions:

$$\frac{\mu u}{K}+\frac{\rho C_F}{\sqrt{K}}u^2+\sigma B_0^2 u = -\frac{\partial P}{\partial x}+\rho\beta g(T-T_c)\cos\emptyset \tag{3.2}$$

$$\frac{\mu v}{K}+\frac{\rho C_F}{\sqrt{K}}v^2+\sigma B_0^2 v = -\frac{\partial P}{\partial y}+\rho\beta g(T-T_c)\sin\emptyset \tag{3.3}$$

The energy equation:

$$u\frac{\partial T}{\partial x}+v\frac{\partial T}{\partial y}=\frac{k}{\rho c_p}\left(\frac{\partial^2 T}{\partial x^2}+\frac{\partial^2 T}{\partial y^2}\right)+\frac{\nu}{Kc_p}u\left(u+\frac{C_F\sqrt{K}}{\nu}u^2\right)+\frac{\sigma B_0^2}{\rho c_p}u^2 \tag{3.4}$$

Where x and y are the inclination coordinates, and the corresponding velocities are u and v respectively, the gravitational acceleration g is acting downward in the direction opposite to the y coordinate.

The Darcy effect is introduced through the term $(\frac{\mu u}{K})$ in the momentum equation. The non-Darcy effect is introduced through the Forchheimer term $(\frac{\rho C_F}{\sqrt{K}}u^2)$ in the momentum equation in x and y-directions. The magnetic effect is introduced into the governing equations through two terms $(\sigma B_0^2 u)$ and $(\sigma B_0^2 v)$ in the momentum equation in x and y-directions, respectively. The viscous heating effect is introduced into the governing equations through the term $(\frac{\nu}{Kc_p}u\left(u+\frac{C_F\sqrt{K}}{\nu}u^2\right))$ in the energy equation. The Joule heating effect is introduced through the term $(\frac{\sigma B_0^2}{\rho c_p}u^2)$ in the energy equation. The convection heat transfer effect is introduced into the governing equations through two terms $(\rho\beta g(T-T_c)\cos\emptyset)$ and $(\rho\beta g(T-T_c)\sin\emptyset)$ in the momentum equation in x and y-directions.

3.3 Boundary condition:

The boundary conditions for the flow in the enclosure are:

1. One wall of the enclosure is kept at uniform high temperature and the opposite is kept at a uniform low temperature.

$$T = T_H \qquad \text{at } x = 0$$

$$T = T_C \qquad \text{at } x = W \tag{3.5}$$

where W is the width of the enclosure as shown in figure (3.1).

2. The other two walls of the enclosure are adiabatic.

$$\frac{\partial T}{\partial y} = 0 \qquad \text{at } y = 0 \text{ and } y = H \tag{3.6}$$

where H is the lingth of the enclosure as shown in figure (3.1).

3. Velocity component normal to wall = 0 on all walls.

$$u = 0 \qquad \text{at } x = 0 \text{ and } x = W$$

$$v = 0 \qquad \text{at } y = 0 \text{ and } y = H \tag{3.7}$$

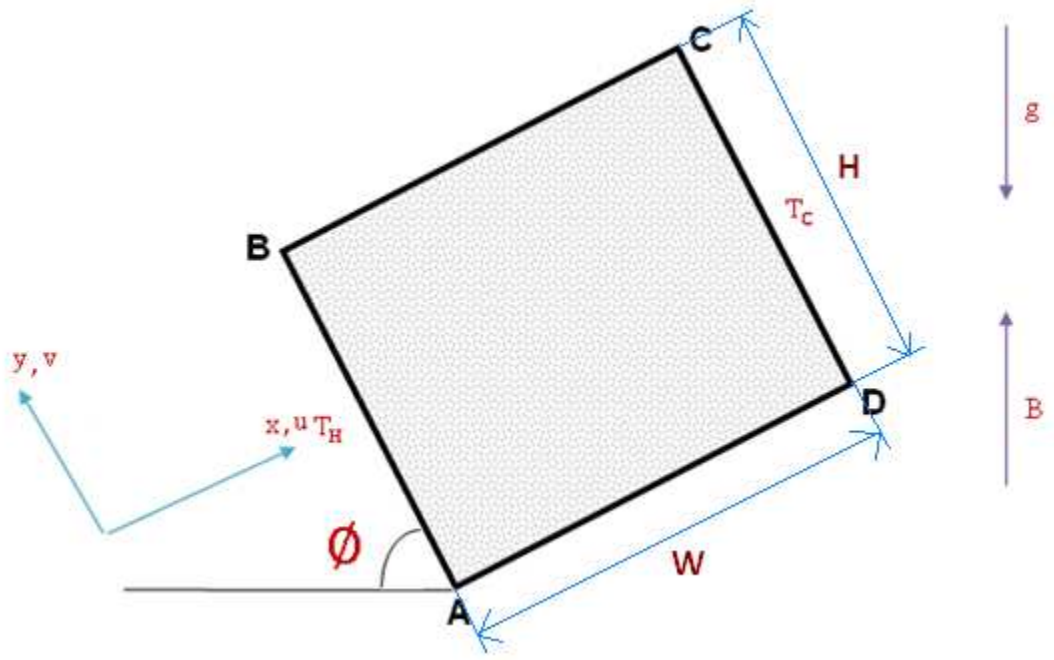

Figure 3.1 Schematic of physical model and coordinate system

3.4 Transforming the case of study into dimensionless form using a set of suitable variables:

The solution will be obtained in terms of the stream function. The stream function is defined by:

$$u = \frac{\partial \psi}{\partial y}, v = -\frac{\partial \psi}{\partial x} \tag{3.8}$$

In terms of the stream function, the continuity equation, i.e., Eq.(3.1), is:

$$\frac{\partial^2 \psi}{\partial x \partial y} - \frac{\partial^2 \psi}{\partial x \partial y} = 0 \tag{3.9}$$

Derivation the momentum equation in x and y-directions, i.e., Eq.(3.2) and (3.3), with respect to y and x respectively and by subtracting the resulting equations, the pressure is eliminated and the following equation is obtained:

$$\frac{\mu}{K}\left(\frac{\partial u}{\partial y}-\frac{\partial v}{\partial x}\right)+\frac{\rho C_F}{\sqrt{K}}\frac{\partial u^2}{\partial y}+\sigma B_0^2\left(\frac{\partial u}{\partial y}-\frac{\partial v}{\partial x}\right)=\rho\beta g\left(\frac{\partial T}{\partial y}\cos\emptyset-\frac{\partial T}{\partial x}\sin\emptyset\right) \quad (3.10)$$

Using the definition of the stream function, Eq. (3.10) becomes:

$$\frac{\partial^2\psi}{\partial x^2}+\frac{\partial^2\psi}{\partial y^2}+\frac{2C_F\sqrt{K}}{\nu}\frac{\partial\psi}{\partial y}\frac{\partial^2\psi}{\partial y^2}+\frac{K\sigma B_0^2}{\mu}\left(\frac{\partial^2\psi}{\partial y^2}+\frac{\partial^2\psi}{\partial x^2}\right)$$
$$=\frac{\rho\beta gK}{\mu}\left(\frac{\partial T}{\partial y}\cos\emptyset-\frac{\partial T}{\partial x}\sin\emptyset\right) \quad (3.11)$$

In terms of the stream function, the energy equation, i.e., Eq.(3.4), is:

$$\frac{\partial\psi}{\partial y}\frac{\partial T}{\partial x}-\frac{\partial\psi}{\partial x}\frac{\partial T}{\partial y}=\frac{k}{\rho c_p}\left(\frac{\partial^2 T}{\partial x^2}+\frac{\partial^2 T}{\partial y^2}\right)+\frac{\nu}{Kc_p}\frac{\partial\psi}{\partial y}\left(\frac{\partial\psi}{\partial y}+\frac{C_F\sqrt{K}}{\nu}\left(\frac{\partial\psi}{\partial y}\right)^2\right)$$
$$+\frac{\sigma B_0^2}{\rho c_p}\left(\frac{\partial\psi}{\partial y}\right)^2 \quad (3.12)$$

Equations (3.11) and (3.12) will be written in dimensionless form. For this purpose, the following dimensionless variables are defined:

$$X=\frac{x}{W}, Y=\frac{y}{W}$$

$$\Psi=\frac{\psi}{\alpha_a}, \theta=\frac{T-T_C}{T_H-T_C} \quad (3.13)$$

Where, as before, the apparent thermal diffusivity of the porous material, α_a, is equal to $\left(\frac{k}{\rho c_p}\right)$.

In terms of variables defined in Eq. (3.13), Eq. (3.11) and (3.12) become:

$$\frac{\partial^2\Psi}{\partial X^2}+\frac{\partial^2\Psi}{\partial Y^2}+2Fr\frac{\partial\Psi}{\partial Y}\frac{\partial^2\Psi}{\partial Y^2}+Ha^2\left(\frac{\partial^2\Psi}{\partial Y^2}+\frac{\partial^2\Psi}{\partial X^2}\right)=$$

$$Ra_w\left(\frac{\partial\theta}{\partial Y}\cos\emptyset-\frac{\partial\theta}{\partial X}\sin\emptyset\right) \qquad (3.14)$$

$$\frac{\partial\Psi}{\partial Y}\frac{\partial\theta}{\partial X}-\frac{\partial\Psi}{\partial X}\frac{\partial\theta}{\partial Y}=\frac{\partial^2\theta}{\partial X^2}+\frac{\partial^2\theta}{\partial Y^2}+Ge\frac{\partial\Psi}{\partial Y}\left(\frac{\partial\Psi}{\partial Y}+Fr\left(\frac{\partial\Psi}{\partial Y}\right)^2\right)$$

$$+(Ge)(Ha^2)\left(\frac{\partial\Psi}{\partial Y}\right)^2 \qquad (3.15)$$

Where Ra_w is the modified Rayleigh number based on the enclosure width W, i.e.:

$$Ra_w=\frac{\beta gK(T_H-T_C)W}{\alpha_a\nu} \qquad (3.16)$$

here Fr is the Forchheimer number based on the enclosure width W, i.e.:

$$Fr=\frac{C_F\alpha_a\sqrt{K}}{\nu W} \qquad (3.17)$$

Ha^2 is the magnetic influence number, i.e.:

$$Ha^2=\frac{K\sigma B_0^2}{\mu} \qquad (3.18)$$

and Ge is the Gebhart number, i.e.:

$$\mathrm{Ge} = \frac{\nu \alpha_a}{\mathrm{K} c_p (T_H - T_C)} \tag{3.19}$$

In terms of dimensionless variables defined in Eq. (3.13), the boundary conditions are:

1. Isothermal walls

$$\theta = 1 \qquad \text{at } X = 0$$

$$\theta = 0 \qquad \text{at } X = 1 \tag{3.20}$$

2. Adiabatic walls

$$\frac{\partial \theta}{\partial Y} = 0 \qquad \text{at } Y = 0 \text{ and } Y \tag{3.21}$$

Here A=H/W is the so-called aspect ratio of the enclosure.

In terms of the stream function, the boundary conditions on the velocity component normal to wall are:

$$\frac{\partial \psi}{\partial y} = 0 \qquad \text{at } x = 0 \text{ and } x = W$$

$$\frac{\partial \psi}{\partial x} = 0 \qquad \text{at } y = 0 \text{ and } y = H \tag{3.22}$$

But the absolute value of the stream function is quite arbitrary because it is only derivatives that occur in the governing equations. Hence, it will arbitrarily be assumed that the stream function has a value of 0 at the point A shown in fig. (3.1). The boundary conditions indicate that $\partial\psi/\partial y$ is 0 along AB. Hence, ψ is 0 at point A, it is zero everywhere along AB. Along BC the boundary conditions indicate that $\partial\psi/\partial x = 0$. Hence, since ψ is 0 at point B, it is zero everywhere along BC. In similar way, it can be deduced that ψ is 0 everywhere along CD and DA. Hence, along all

of ABCD, ψ is 0 if it is arbitrary taken as 0 at point A. Hence, the boundary condition on the stream function is:

$$\text{All wall surfaces } \psi = 0 \tag{3.23}$$

In terms of dimensionless variables defined in Eq. (3.13), the boundary condition on the stream function is:

$$\text{On all wall surfaces } \Psi = 0 \tag{3.24}$$

Equations (3.14) and (3.15) with corresponding boundary conditions (3.20), (3.21), (3.22) and (3.24) are giving to be solved numerically using finite difference technique for both the stream function and the dimensionless temperature.

Chapter 4

Numerical Solution

4.1 Introduction:

In recent years a large number of numerical methods have been developed for the solving of boundary layer equations, such as the finite difference method, Galerkin method, and finite element method. Of these, the finite difference method is at present the most common for boundary layer equations. In the finite difference approach, the dependent variables are considered to exist only at discrete points. Derivatives are approximated by finite difference resulting in an algebraic representation of the partial differential equation. Many different finite difference representations are possible for any given partial differential equation.

4.2 Finite difference scheme:

In this chapter, finite difference numerical procedure, basically identical to that used before to solve for a flow in a fluid-filled enclosure, will be discussed. The solution of equations by this method can be obtained by write the difference equations by using central differences. If a uniformly spaced grid is used and if attention is directed to the grid points, as shown in fig.(4.1), the following finite-difference form of Eq. (3.15) is obtained:

$$\left[\frac{\Psi_{i,j+1}-\Psi_{i,j-1}}{2\Delta Y}\right]\left[\frac{\theta_{i+1,j}-\theta_{i-1,j}}{2\Delta X}\right]-\left[\frac{\Psi_{i+1,j}-\Psi_{i-1,j}}{2\Delta X}\right]\left[\frac{\theta_{i,j+1}-\theta_{i,j-1}}{2\Delta Y}\right]=\left[\frac{\theta_{i+1,j}-2\theta_{i,j}+\theta_{i-1,j}}{\Delta X^2}\right]+\left[\frac{\theta_{i,j+1}-2\theta_{i,j}+\theta_{i,j-1}}{\Delta Y^2}\right]+$$

$$\mathrm{Ge}\left[\frac{\Psi_{i,j+1}-\Psi_{i,j-1}}{2\Delta Y}\right]\left[\left[\frac{\Psi_{i,j+1}-\Psi_{i,j-1}}{2\Delta Y}\right]+\mathrm{Fr}\left[\frac{\Psi_{i,j+1}-\Psi_{i,j-1}}{2\Delta Y}\right]^2\right]+(\mathrm{Ge})(\mathrm{Ha}^2)\left[\frac{\Psi_{i,j+1}-\Psi_{i,j-1}}{2\Delta Y}\right]^2 \quad (4.1)$$

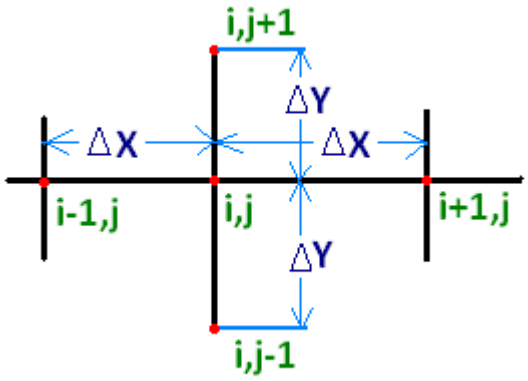

Fig. 4.1 Nodal points used.

An iterative procedure is actually used in which the values of the variables at nodal points are first guessed. Updated values are then obtained by applying the governing equations and the process is repeated until convergence is attained. For this reason, Eq. (4.1) is written as:

$$\theta_{i,j} = \left\{\left(\frac{\theta_{i+1,j}+\theta_{i-1,j}}{\Delta X^2}\right)+\left(\frac{\theta_{i,j+1}+\theta_{i,j-1}}{\Delta Y^2}\right)+(Ge)(Ha^2)\left(\frac{\Psi_{i,j+1}-\Psi_{i,j-1}}{2\Delta Y}\right)^2\right.$$

$$+\,Ge\left(\frac{\Psi_{i,j+1}-\Psi_{i,j-1}}{2\Delta Y}\right)\left[\left(\frac{\Psi_{i,j+1}-\Psi_{i,j-1}}{2\Delta Y}\right)+Fr\left(\frac{\Psi_{i,j+1}-\Psi_{i,j-1}}{2\Delta Y}\right)^2\right]$$

$$\left.+\left(\frac{\Psi_{i+1,j}-\Psi_{i-1,j}}{2\Delta X}\right)\left(\frac{\theta_{i,j+1}-\theta_{i,j-1}}{2\Delta Y}\right)-\left(\frac{\Psi_{i,j+1}-\Psi_{i,j-1}}{2\Delta Y}\right)\left(\frac{\theta_{i+1,j}-\theta_{i-1,j}}{2\Delta X}\right)\right\}\Big/\left(\frac{2}{\Delta X^2}+\frac{2}{\Delta Y^2}\right) \tag{4.2}$$

The right-hand side of this equation is calculated using the "most recent" values of the variables. Under-relaxation is actually used so the updated value of θ is given by:

$$\theta_{i,j}^{1} = \theta_{i,j}^{0} + r\left(\theta_{i,j}^{calc} - \theta_{i,j}^{0}\right) \tag{4.3}$$

Where $\theta_{i,j}^{calc}$ is the value given by Eq. (4.2) and $\theta_{i,j}^{0}$ is the value of $\theta_{i,j}$ at the previous iteration.

Eq. (4.2) is applied at all "internal" nodal points, i.e., at all points within the enclosure. The boundary conditions determine the dimensionless temperatures on the walls. These give:

$$j = 1,2,\dots,N:\ \ \theta_{1,j} = 1, \theta_{M,j} = 0 \tag{4.4}$$

There being N nodal points in Y-direction and M in X-direction. On the other two walls, since the gradient in the Y-direction is zero, to first order accuracy:

$$i = 1,2,\dots,M:\qquad \theta_{i,1} = \theta_{i,2},\ \ \theta_{i,N} = \theta_{i,N-1} \tag{4.5}$$

The stream function equation, i.e., Eq.(3.14), is treated in the same way as the energy equation. The following finite-difference form of Eq. (3.14) is, therefore, obtained:

$$\left[\frac{\Psi_{i,j+1}-2\Psi_{i,j}+\Psi_{i,j-1}}{\Delta Y^2}\right] + \left[\frac{\Psi_{i+1,j}-2\Psi_{i,j}+\Psi_{i-1,j}}{\Delta X^2}\right] + 2Fr\left[\frac{\Psi_{i,j+1}-\Psi_{i,j-1}}{2\Delta Y}\right]\left[\frac{\Psi_{i,j+1}-2\Psi_{i,j}+\Psi_{i,j-1}}{\Delta Y^2}\right] +$$

$$Ha^2\left[\frac{\Psi_{i,j+1}-2\Psi_{i,j}+\Psi_{i,j-1}}{\Delta Y^2} + \frac{\Psi_{i+1,j}-2\Psi_{i,j}+\Psi_{i-1,j}}{\Delta X^2}\right] = Ra_w\left[\frac{\theta_{i,j+1}-\theta_{i,j-1}}{2\Delta Y}\cos\emptyset - \frac{\theta_{i+1,j}-\theta_{i-1,j}}{2\Delta X}\sin\emptyset\right] \tag{4.6}$$

$$\Psi_{i,j} = \left\{\left(\frac{\Psi_{i,j+1}+\Psi_{i,j-1}}{\Delta Y^2}\right) + \left(\frac{\Psi_{i+1,j}+\Psi_{i-1,j}}{\Delta X^2}\right) + 2Fr\left(\frac{\Psi_{i,j+1}-\Psi_{i,j-1}}{2\Delta Y}\right)\left(\frac{\Psi_{i,j+1}+\Psi_{i,j-1}}{\Delta Y^2}\right)\right.$$

$$+Ha^2\left(\frac{\Psi_{i,j+1}+\Psi_{i,j-1}}{\Delta Y^2} + \frac{\Psi_{i+1,j}+\Psi_{i-1,j}}{\Delta X^2}\right) - Ra_w\left(\frac{\theta_{i,j+1}-\theta_{i,j-1}}{2\Delta Y}\cos\emptyset -\right.$$

$$\left.\left.\frac{\theta_{i+1,j}-\theta_{i-1,j}}{2\Delta X}\sin\emptyset\right)\right\} \Big/ \left\{\frac{2}{\Delta Y^2} + \frac{2}{\Delta X^2} + \frac{2Fr}{\Delta Y^2}\left(\frac{\Psi_{i,j+1}-\Psi_{i,j-1}}{\Delta Y}\right) + \frac{2Ha^2}{\Delta X^2}\sin\emptyset + \frac{2Ha^2}{\Delta Y^2}\cos\emptyset\right\} \tag{4.7}$$

The right-hand side of this equation is again calculated using the "most" recent vues of the variables. Under-relaxation is also again used so the updated value of i, j is actually given by:

$$\Psi_{i,j}^1 = \Psi_{i,j}^0 + r\left(\Psi_{i,j}^{calc} - \Psi_{i,j}^0\right) \tag{4.8}$$

Where $\Psi_{i,j}^{calc}$ is the value given by Eq. (4.7) and $\Psi_{i,j}^0$ is the value of $\Psi_{i,j}$ at the previous iteration. r(< 1) is again the under-relaxation parameter.

Eq. (4.7) is applied at all "internal" nodal points. The boundary conditions have the value of $\Psi = 0$ on all boundary points, i.e.:

$$j = 1,2,\dots,N: \quad \Psi_{i,j} = 0,1, \Psi_{M,j} = 0$$

$$i = 1,2,\dots,M: \qquad \Psi_{i,j} = 0,1, \Psi_{i,N} = 0 \tag{4.9}$$

The above procedure is actually implemented in the following way:

1. The values of $\Psi_{i,j}$ and $\theta_{i,j}$ at all nodal points are first set equal to arbitrary initial values, typically the following are used:

$$\Psi_{i,j} = 0$$

$$\theta_{i,j} = 0 \tag{4.10}$$

The assumed θ distribution is that which would exist if there was no convective motion, i.e., if conduction alone existed. Its use is consistent with the assumed distribution of Ψ which implies that there is no flow in the enclosure.

2. Eq. (4.7) in conjunction with Eq. (4.8) is used to obtain updated values of $\Psi_{i,j}$. Because iteration is being used, this process should really be repeated over and over until values of $\Psi_{i,j}$ corresponding to the initially assumed distribution of θ are obtained. Experience suggests, however, that it is quite adequate to undertake this step just twice.
3. Eq. (4.2) in conjunction with Eq. (4.3) is used to obtain updated values of $\theta_{i,j}$. This step is also undertaken twice.
4. Steps (2) and (3) are repeated over and over until convergence is obtained to a specified accuracy which is 10^{-5}.
5. The heat transfer rate distribution is obtained by applying Fourier's law at the heated and cooled walls, i.e.:

$$q_{w_{1,j}} = \frac{k_a\left(T_{1,j} - T_{2,j}\right)}{\Delta x}$$

$$q_{w_{M,j}} = \frac{k_a\left(T_{M-1,j} - T_{M,j}\right)}{\Delta x} \tag{4.11}$$

6. The local Nusselt number is obtained at the heated and cooled walls, i.e.:

$$Nu_{1,j} = \frac{1 - \theta_{2,j}}{\Delta Y}$$

$$Nu_{M,j} = \frac{\theta_{M-1,j}}{\Delta Y} \tag{4.12}$$

Where Nu is the local Nusselt number based on W and where it has been noted that $\theta_{1,j} = 1$, and $\theta_{M,j} = 0$.

Because uniform grid spacing has been used, the mean Nusselt numbers are given by:

$$\overline{Nu}_H = \frac{\Delta Y}{A}\left(\frac{Nu_{1,1}}{2} + Nu_{1,2} + Nu_{1,3} + \cdots + Nu_{1,N-1} + \frac{Nu_{1,N}}{2}\right)$$

$$\overline{Nu}_C = \frac{\Delta Y}{A}\left(\frac{Nu_{M,1}}{2} + Nu_{M,2} + Nu_{M,3} + \cdots + Nu_{M,N-1} + \frac{Nu_{M,N}}{2}\right) \tag{4.13}$$

4.3 Numerical solution justification:

The results, which had obtained by using finite difference method in this study had compared with some results, which had obtained by P.H. and D.Naylor (1973).

This results shown in fig.(4.2-a) and fig.(4.3-a) are obtained by canceling the magnetic effect, Forchheimer, Joule and viscous heating effects terms so, the results are obtained for ϕ=90°, A = 1, Fr = 0, Ge=0, $Ha^2 = 0$, and $Ra_w = 50$.

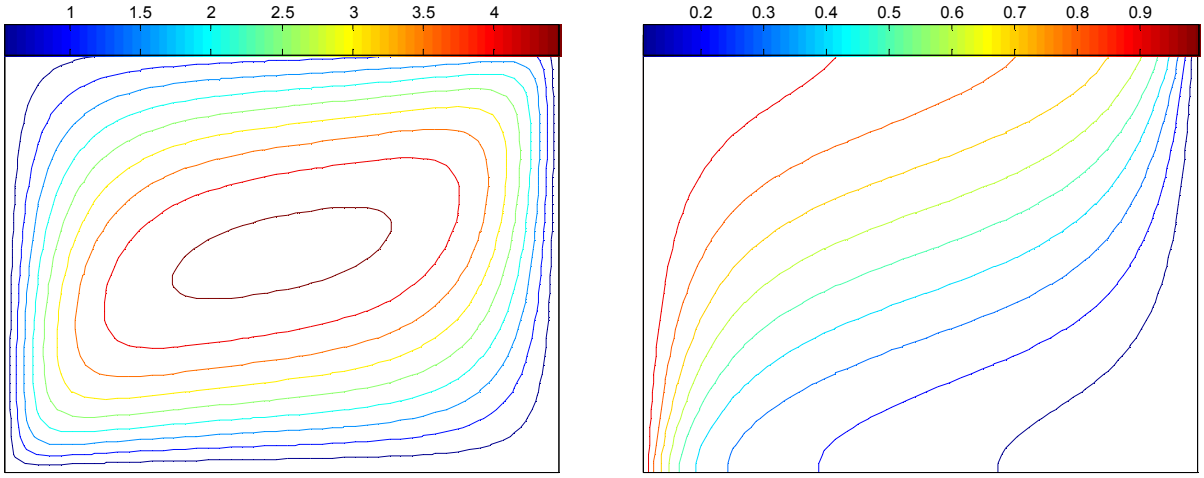

(a)

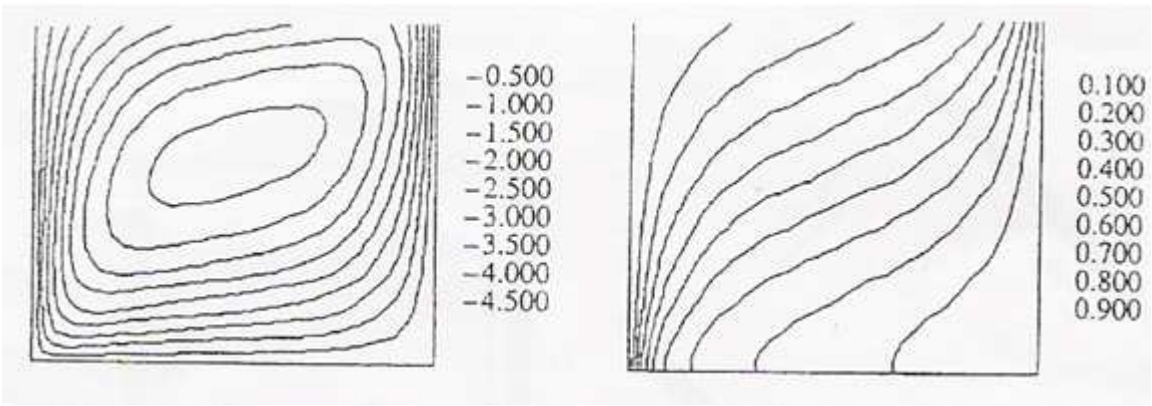

(b)

Fig. 4.2 Typical dimensionless streamline and dimensionless temperature patterns. (a) Present work, (b) P.H. and D.Naylor work.

By comprising the presented results shown in fig.(4.2-a) to the traditional figure shown in fig.(4.2-b) which are obtained for ϕ=90°, A = 1, Fr = 0, Ge=0, $Ha^2 = 0$, and $Ra_w = 50$ it can be seen that the maximum value of dimensionless stream functions are 4.5 for both results, this enhances the presented results in this work. On the other hand, as it is shown, the hot fluid rises up along the left-hand side hot wall and descends along the right-hand side cold wall as seen in fluid isothermal contours which forms a clockwise flow so; the negative sign is coming from the direction of flow.

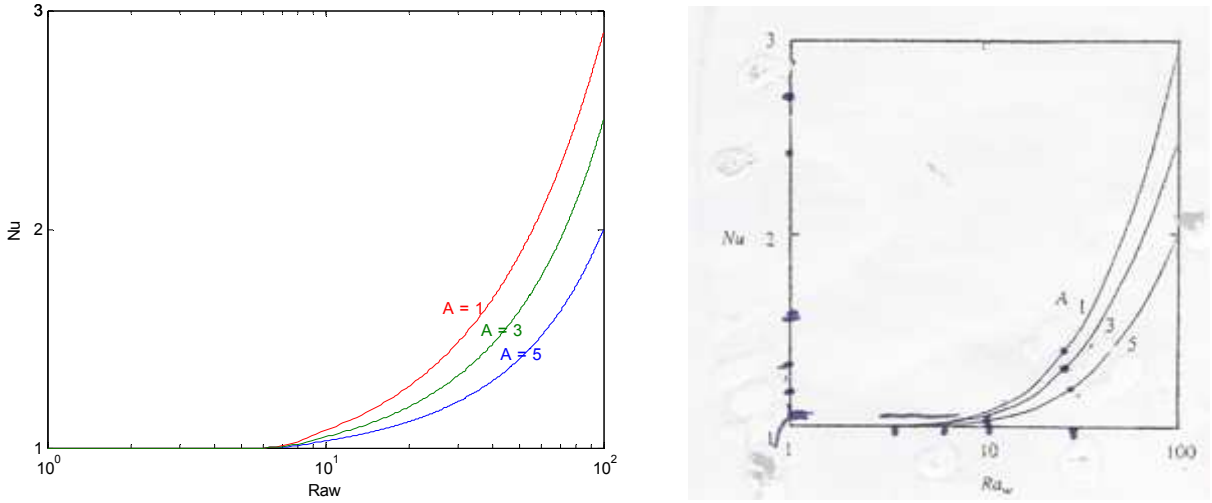

(a) (b)

Fig. 4.3 Variation of mean Nusselt number with Ra_w for various A. (a) Present work, (b) P.H. and D.Naylor work.

and by comparison the present results show in fig.(4.3-a) to the traditional result in fig.(4.3-b) which are obtained for ϕ=90°, A = 1, Fr = 0, Ge=0, $Ha^2 = 0$, and $Ra_w = 50$ it can be seen that the mean Nusselt number have the maximum value at A=1 for both results. So, it can found that the results are identical.

Chapter 5

Results and Discussion

5.1 Introduction:

A numerical study was performed to examine the steady-state, laminar convection heat transfer problem inside a porous media filled inclined rectangular enclosures, the parameters are the magnetic influence number, the Rayleigh number, the Forchheimer number, the inclination angle, the aspect ratio of the enclosure, and the Gebhart number. The left-hand side wall is hot and the right-hand side wall is cold, the other two walls of the enclosure are adiabatic. The Finite difference scheme method is used to solve the momentum and energy equations. The effects of all parameters above are included in the final system of partial differential equations and there effects on the fluid flow and temperature are going to be studied. The dimensionless streamlines and isotherms are plotted to obtain flow patterns and temperature fields at different effects of all parameters above. Also, the effects of all parameters on the mean Nusselt number and the center dimensionless stream are plotted.

5.2 The results without viscous and Joule heating effects (Ge = 0):

5.2.1 Magneto hydrodynamic effects:

The Magneto hydrodynamic effects can be studied by using different values of the magnetic influence number (Ha^2) in the momentum equation for $\emptyset$=30°, A = 1, Fr = 0.01. The results show that the flow and temperature field are very complex. Figure (5.1) illustrates the effect of magnetic influence number on the dimensionless streamlines and isotherms patterns, as it is shown, the hot fluid rises up along the left-hand side hot wall and descends along the right-hand side cold wall as seen in fluid isothermal contours. At $Ha^2 = 0$ the hotter fluid along the left-hand side wall ascends upward and the colder fluid along the right-hand side wall descends downward quickly; due to the usual gravitational buoyancy force, which forms a clockwise flow.

At $Ha^2 = 0.03$ the hot fluid along the left-hand side wall ascends upward and the cold fluid along the right-hand side wall descends downward with smaller dimensionless stream function by comparison with fluid flow at $Ha^2 = 0$. At $Ha^2 = 0.1$ the dimensionless stream function have very small value which is less than 1. By increasing Ha^2 to reach 1, the magnetic force becomes large and the dimensionless stream function of the hot fluid along the left-hand side wall has bigger value than the cold fluid along the right-hand side wall. On the other hand, the fluid in the middle half enclosure has two circulations of flow with bigger dimensionless stream function value by comparison with the flow along the walls. At $Ha^2 = 3$ The hot fluid along the left-hand side wall has circulation of flow with bigger dimensionless stream value by comparison with the cold fluid along the opposite wall and in the middle half of the enclosure. So, by increasing Ha^2 the circulation of flow becomes along the left-hand side wall and the dimensionless stream function is decreasing to reach negligible value; due to the magnetic effect is just reversed to the usual gravitational convection and the heat transfer becomes by conduction; due to decreasing in Nusselt number to reach 1 at $Ha^2 = 4$. Figure (5.2) shows the relation between the variations of mean Nusselt number with magnetic influence number. It can be seen that the mean Nusselt number is decreased by increasing the magnetic influence number; this is due to decreasing in dimensionless temperature in the upper half region along the left-hand side and the lower half region along the right-hand side wall.

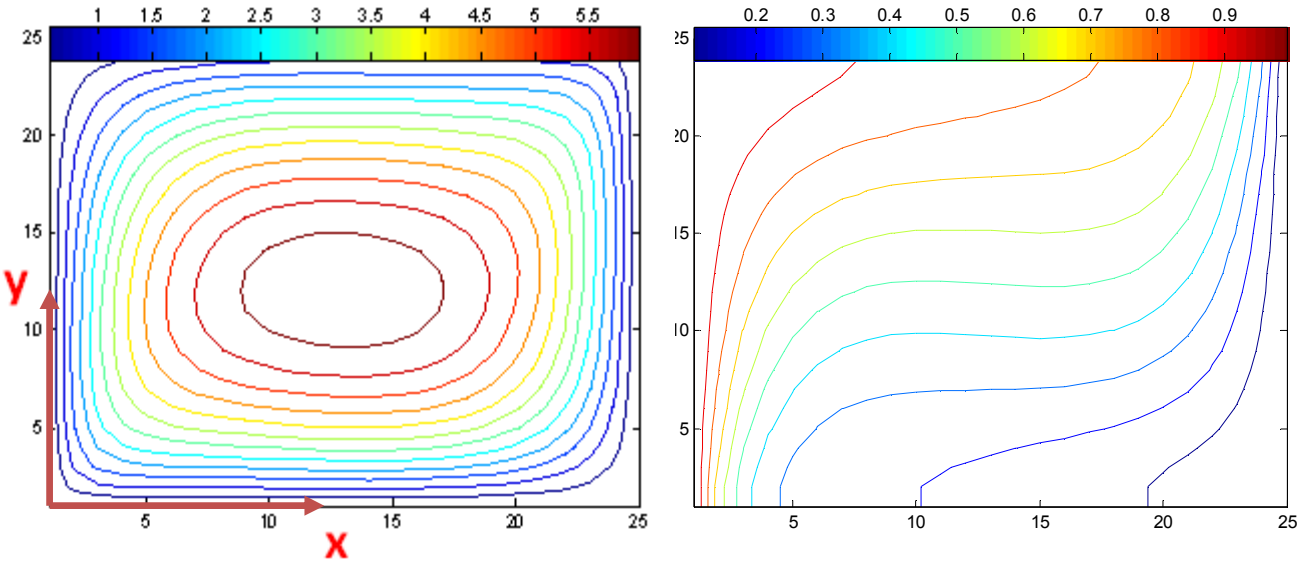

(a)

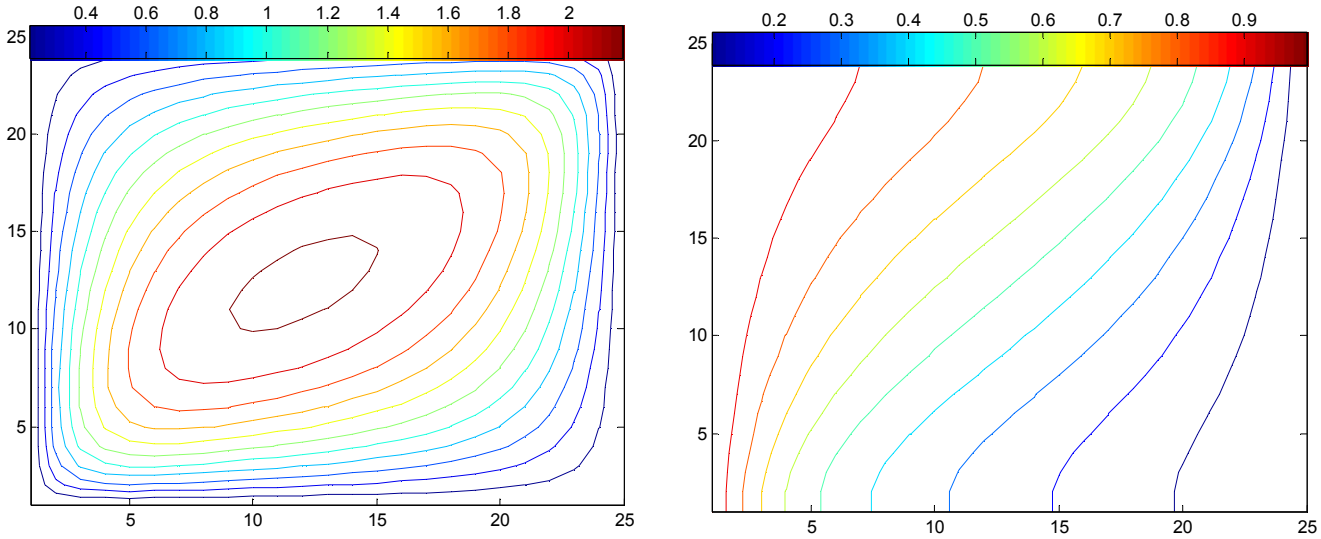

(b)

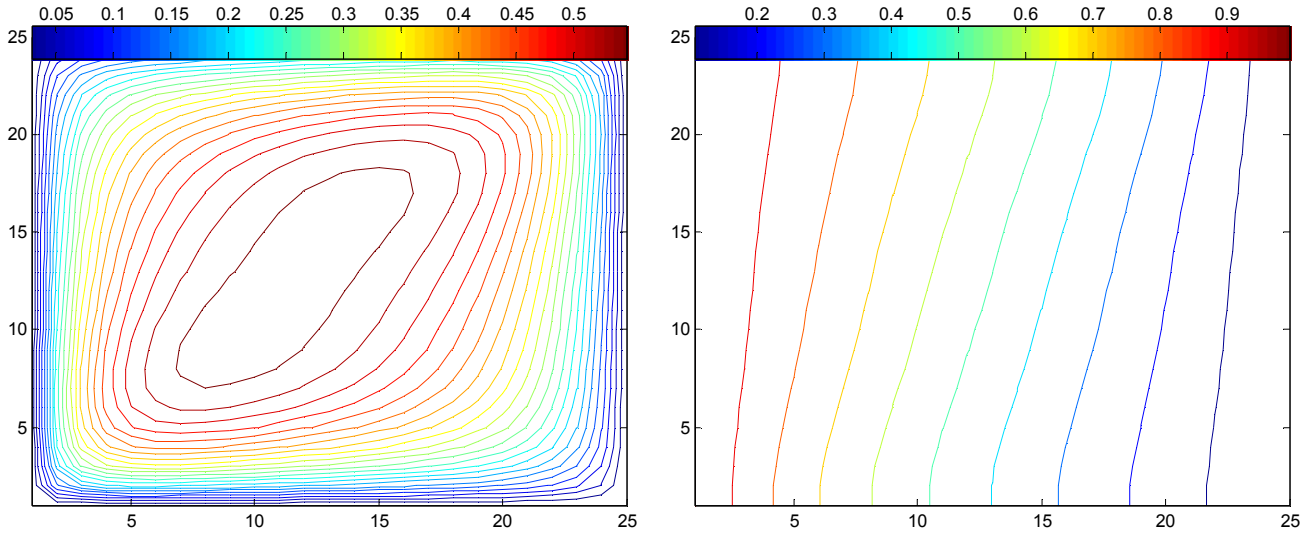

(c)

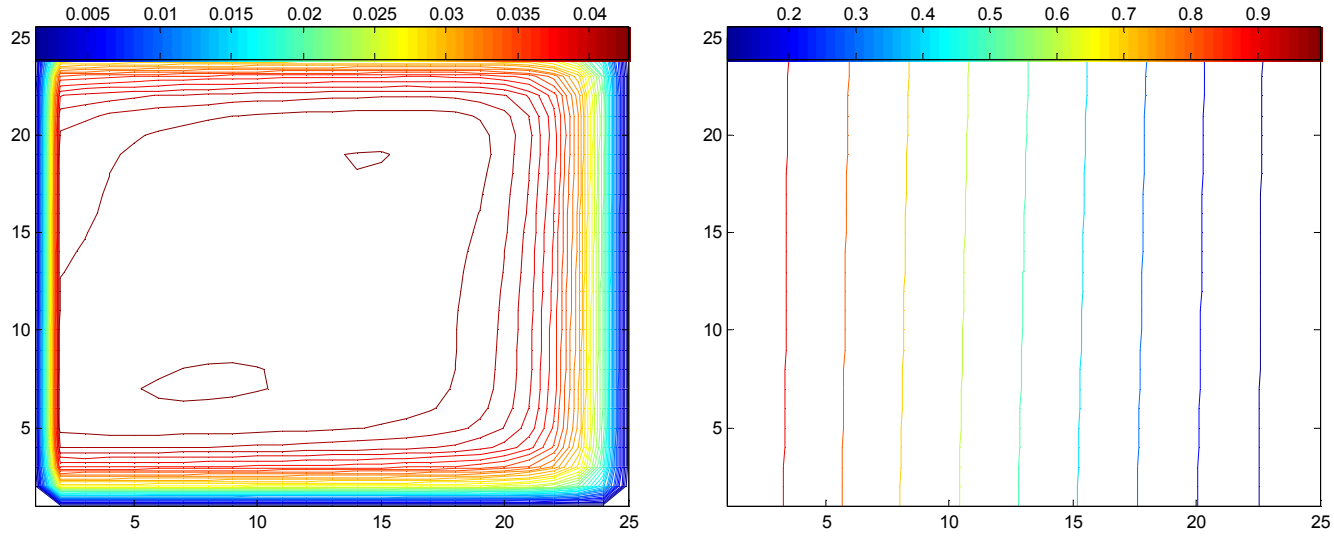

(d)

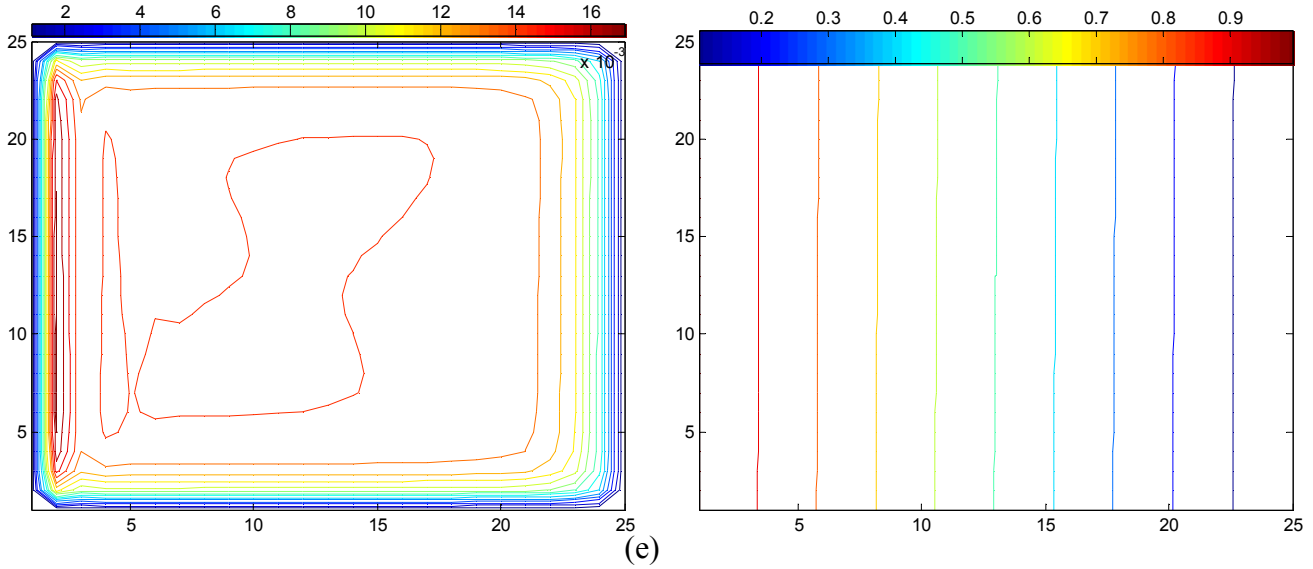

(e)

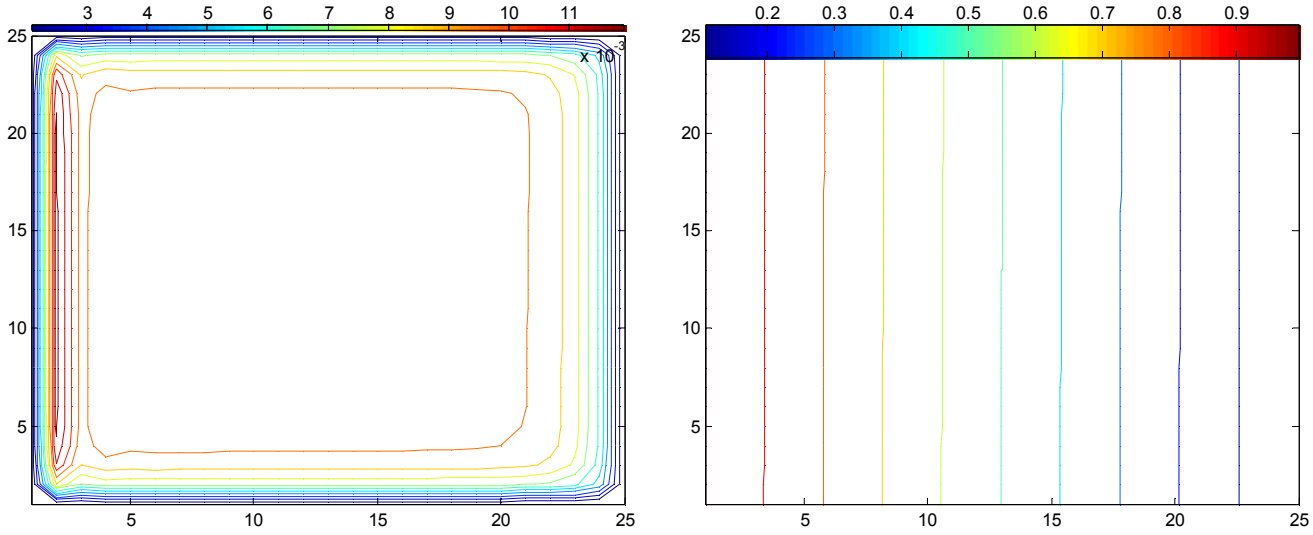

(f)

Fig. 5.1 Typical dimensionless streamline and dimensionless temperature patterns for various magnetic influence number (a) $Ha^2 = 0$, (b) $Ha^2 = 0.03$, (c) $Ha^2 = 0.1$, (d) $Ha^2 = 1$, (e) $Ha^2 = 3$, (f) $Ha^2 = 4$ for Ø=30°, A = 1, Fr = 0.01, and $Ra_w = 100$

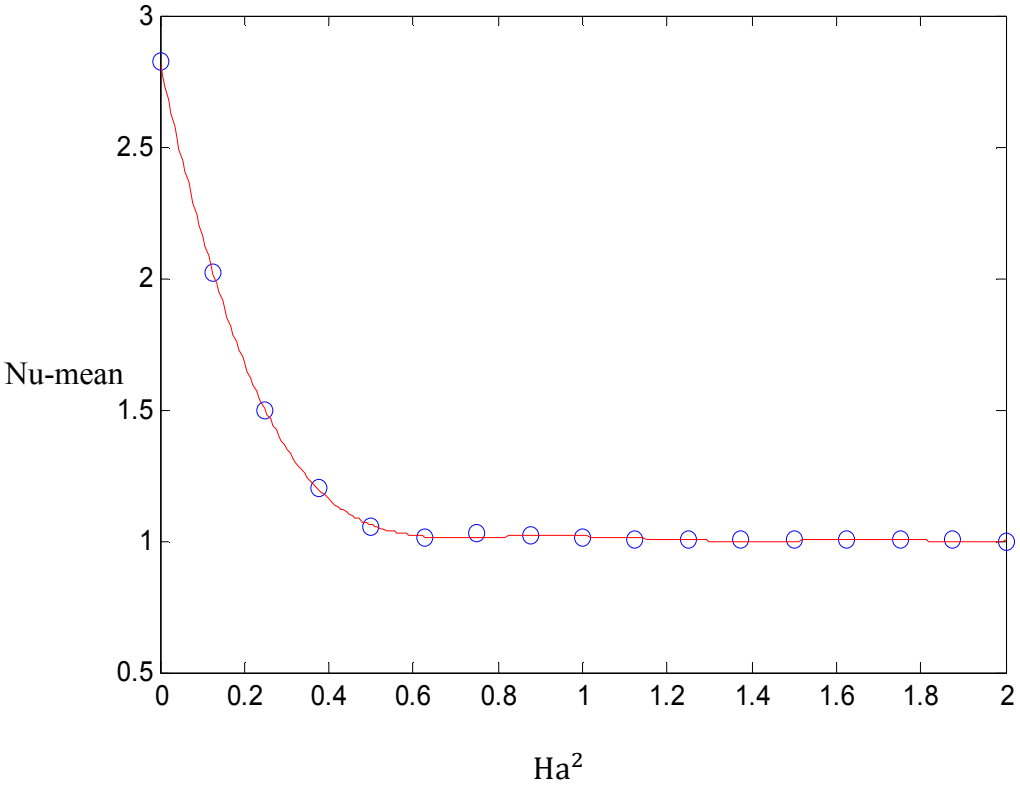

Fig. 5.2 Variation of Nu-mean with Ha^2 for an enclosure for Ø=30°, A = 1, Fr = 0.01, and Ra_w = 100

5.2.2 The Modified Rayleigh number effects:

Figures (5.3) illustrates the effect of Rayleigh number in the momentum equation on the dimensionless streamlines and isotherms patterns with other parameters unchanged, as it is shown, Rayleigh number has a certain effect on the heat transfer and fluid flow. When the Rayleigh number is small, the magnitude of magnetic force has little effect on the heat transfer rate. At $Ra_w = 1$ the hot fluid along the left-hand side wall and the cold fluid along the right-hand side wall have small value of dimensionless stream function of fluid flow, which is 0.015 at the centre of the enclosure and the heat transfer becomes by conduction. By increasing Ra_w to reach the maximum value which is 100, the magnetic force has the largest effect on the heat transfer rate and the value of dimensionless stream line reaches 3 at $Ha^2 = 0.02$ at the centre of the enclosure. The values of the mean Nusselt number are shown in Fig. (5.4). It is found that, When the Rayleigh number is small, the value of mean Nusselt number is 1; this is due to negligible convection heat transfer effects when $Ra_w \rightarrow 0$ and the value of Nu-mean = 1 means a pure conduction heat transfer problem. It can be seen also, the mean Nusselt number is increased to reach the maximum value at $Ra_w = 100$; this is due to increasing in convection heat transfer when the Modified Rayleigh number is increased.

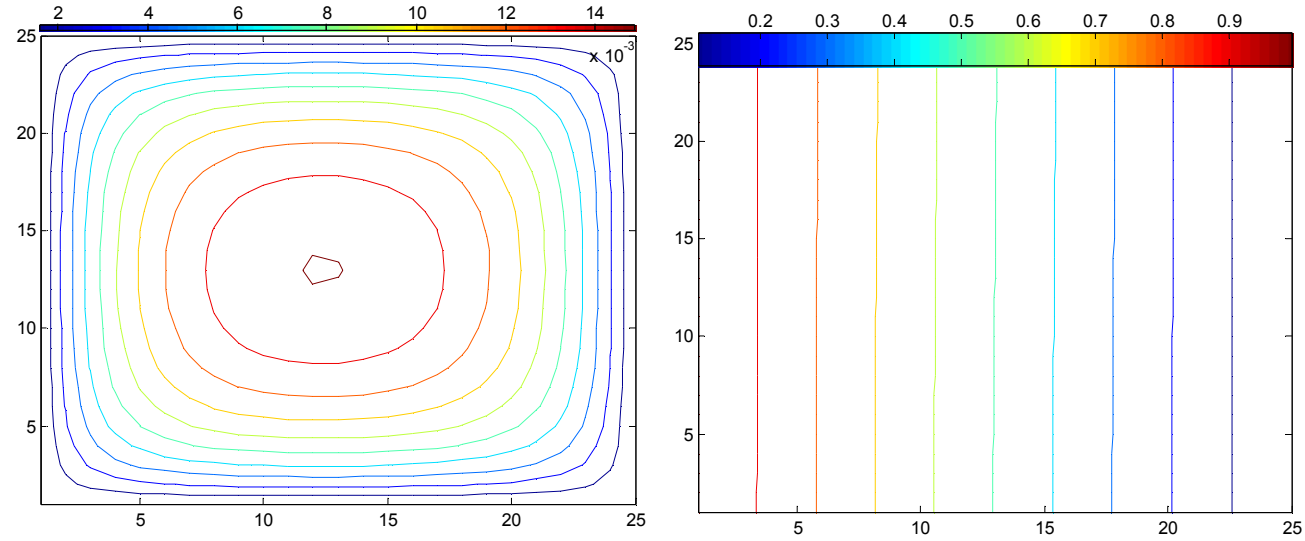

(a)

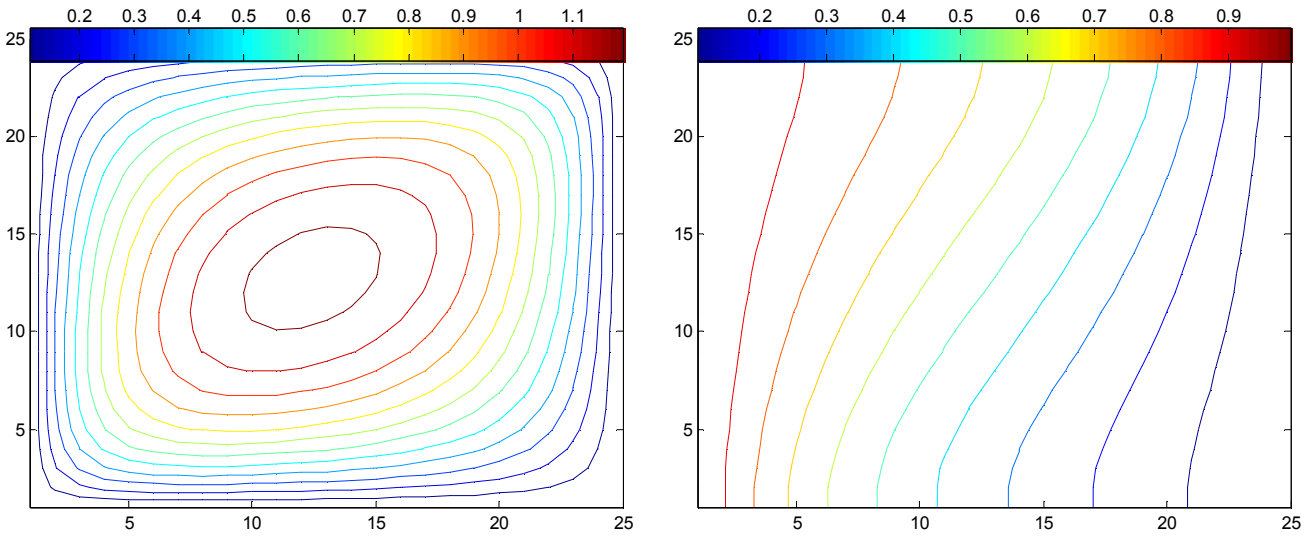

(b)

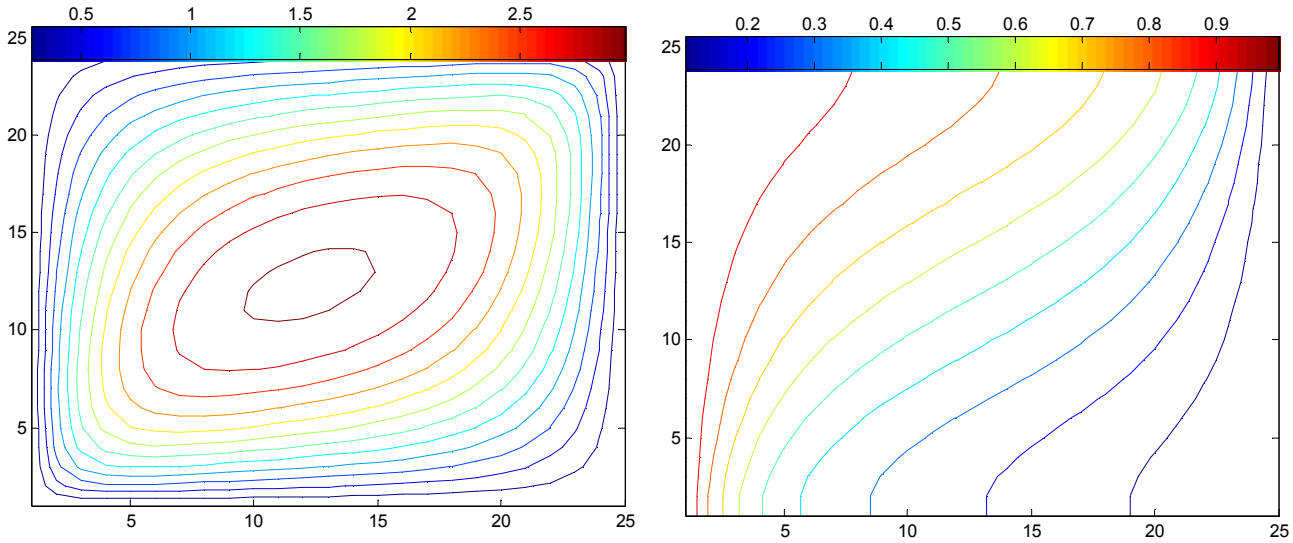

(c)

Fig. 5.3 Typical dimensionless streamline and dimensionless temperature patterns for various Darcy-modified Rayleigh number (a) $Ra_w = 1$, (b) $Ra_w = 50$, (c) $Ra_w = 100$, for ∅=30°, A = 1, Fr = 0.01, and $Ha^2 = 0.02$

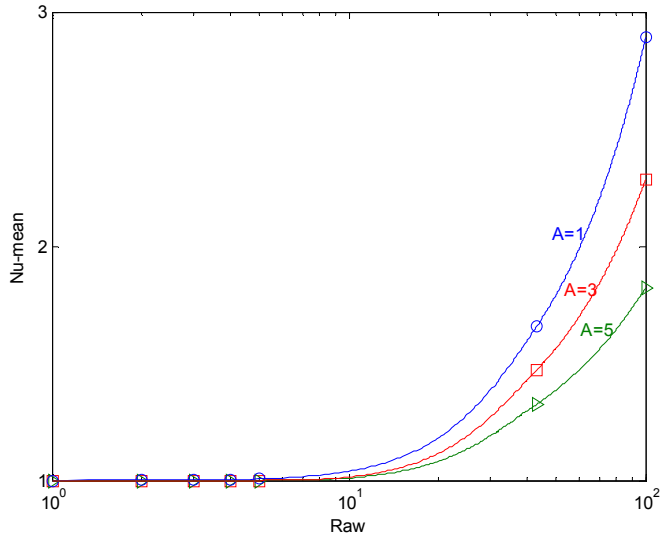

Fig. 5.4 Variation of Nu-mean with Raw for an enclosure for various A for ∅=30°, Fr = 0.01, and $Ha^2 = 0.02$

5.2.3 The inclination angle of the enclosure effects:

In order to examine the effects of inclination angle, computations are carried out for a fluid with different values of the inclined angle; while other geometric parameters remained unchanged. Numerical results are obtained for (Ra_w = 100, A = 1, Ha^2 = 0.02, and Fr = 0.01). Figure (5.5) illustrates the effect of the inclination angle of the enclosure on the dimensionless streamlines and isotherms patterns with other parameters unchanged, as it is shown, $\emptyset$ has a certain effect on the heat transfer and fluid flow. When $\emptyset = 0$ the hotter fluid along the left-hand side wall descends downward and the colder fluid along the right-hand side wall ascends upward due to the usual gravitational buoyancy force, which forms a counterclockwise flow. At $\emptyset = 30°$ the circulation of fluid becomes clockwise flow as well as $\emptyset = 90°$; this is due to decreasing in the gravitational buoyancy force by increasing the angle of inclination. At $\emptyset = 30°$ the fluid flow have the largest dimensionless streamline function by comparison with the flow at any value of $\emptyset$. At $\emptyset = 180°$ the magnitude of magnetic force has not effect on the heat transfer rate. The hot fluid along the left-hand side wall and the cold fluid along the right-hand side wall have not flow when $\emptyset = 180°$; this is due to the location of the hot wall which becomes at the upper portion of the enclosure. Figure (5.6 and 5.7) show the relation between the variation of mean Nusselt number and dimensionless center-stream function with angle of inclination for an enclosure for various Ha^2 and Ra_w, respectively. It can be seen that at $\emptyset = 30°$ the mean Nusselt number and dimensionless center-stream function have maximum values. On the other hand, it can be seen that the dimensionless center-stream function is decreased by increasing the magnetic influence number and it is increased by increasing the Rayleigh number.

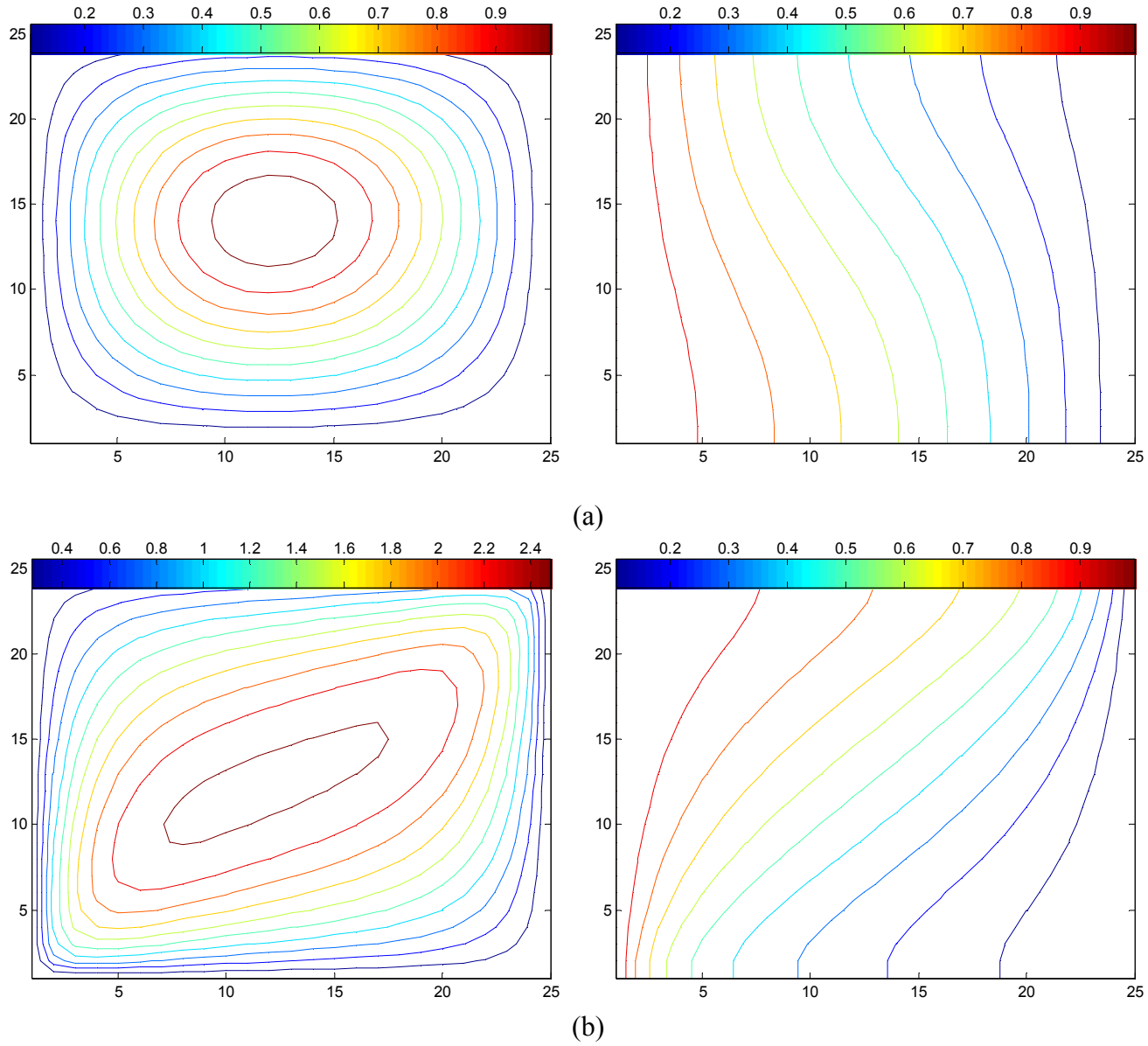

Fig. 5.5 Typical dimensionless streamline and dimensionless temperature patterns for various inclination angle of the enclosure (a) $\emptyset = 0$, (b) $\emptyset = 90°$ for $Ra_w = 100$, A = 1, Fr = 0.01, and $Ha^2 = 0.02$

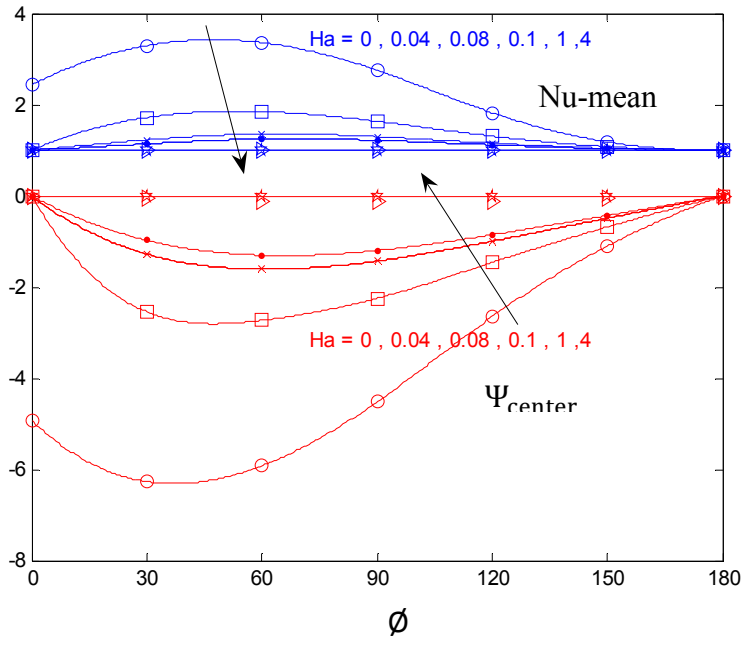

Fig. 5.6 Variation of mean Nusselt number and dimensionless center-stream function with angle of inclination for an enclosure for various Ha^2 for $Ra_w = 100$, A = 1, Fr = 0.01

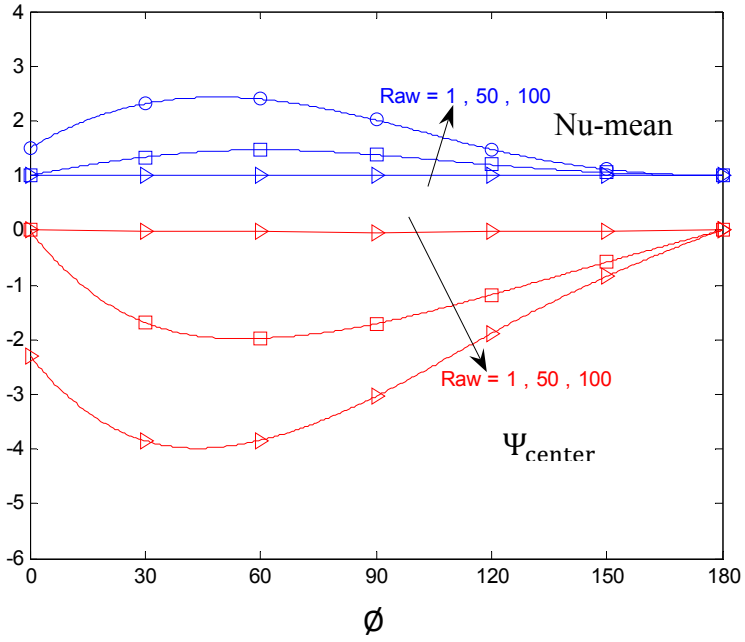

Fig. 5.7 Variation of mean Nusselt number and dimensionless center-stream function with angle of inclination for an enclosure for various Ra_w for A = 1, Fr = 0.01, and $Ha^2 = 0.02$

5.2.4 The aspect ratio of the enclosure effects:

Figure (5.8) illustrates the effect of aspect ratio of the enclosure on the dimensionless streamlines isotherms with other parameters unchanged, as it is shown, it is found that, When A=0.4,0.6, and 1 the fluid is rotating around the centre of the enclosure. At A=3, 5 the fluid has two and four circulations of flow, respectively. On the other hand, when the aspect ratio less than or equal 1 the heat transfer will be increased; this is due to small distance between the two boundaries and increasing in the dimensionless temperature at the upper left-hand side and the lower right-hand side, by increasing the aspect ratio to become bigger than 1 the heat transfer will be decreased; this is due to increasing in the length of the enclosure and the fluid has more than one circulation of flow therefore; the dimensionless temperature at the upper left-hand side and the lower right-hand side are decreased. So, the dimensionless stream function and the Nusselt number are increased when the aspect ratio less than 1 and decreased when the aspect ratio bigger than 1.

The values of the mean Nusselt number are shown in Figure (5.4) for A=1, 3, and 5. It can be seen that the heat transfer is decreased with the increasing of aspect ratio.

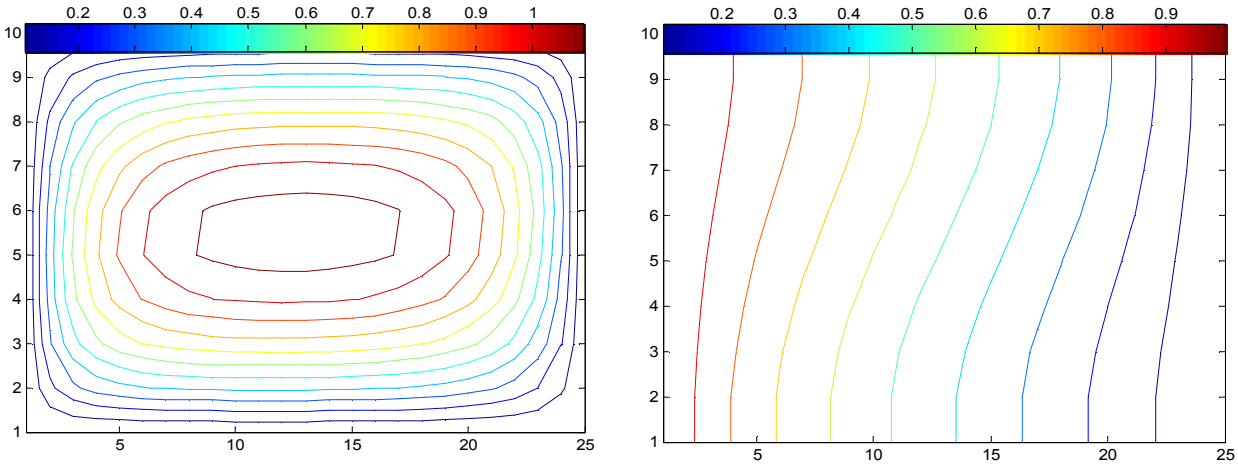

(a)

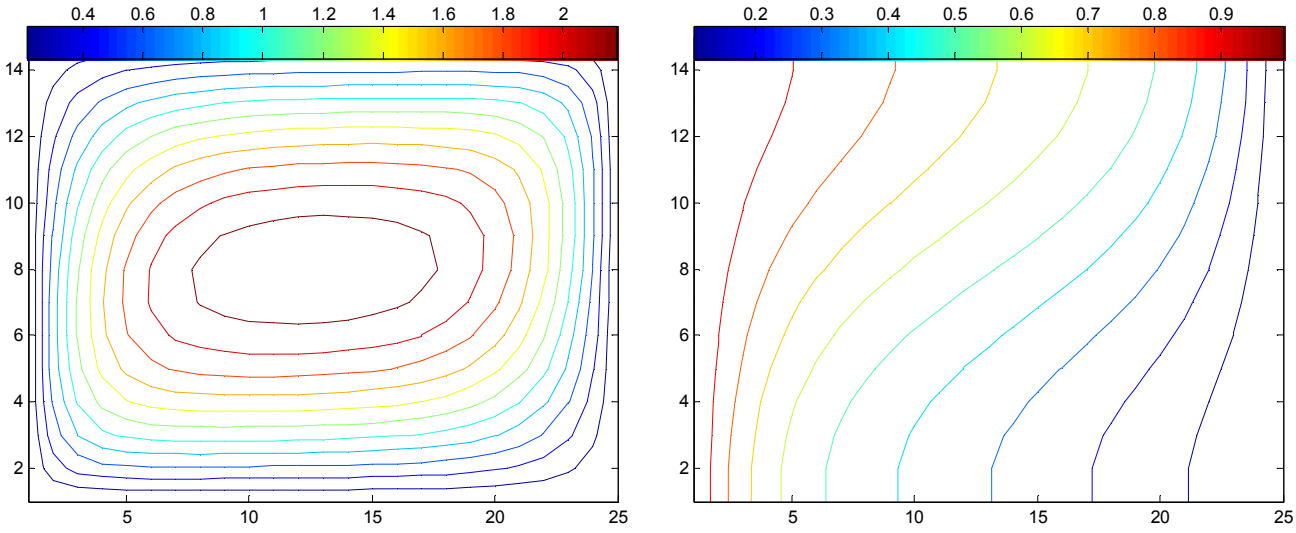

(b)

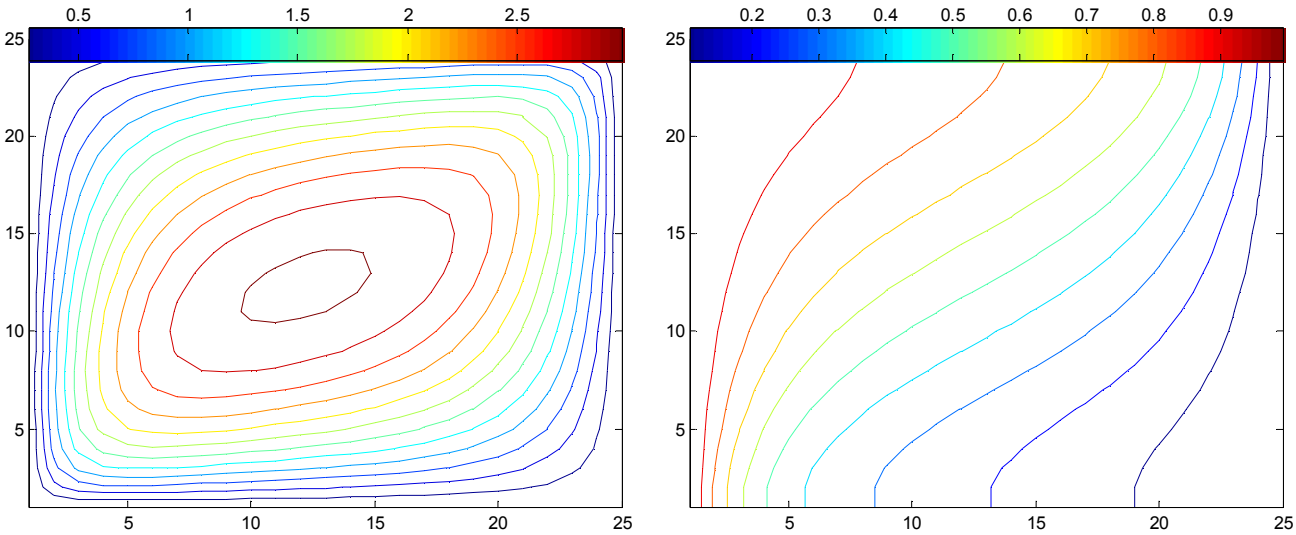

(c)

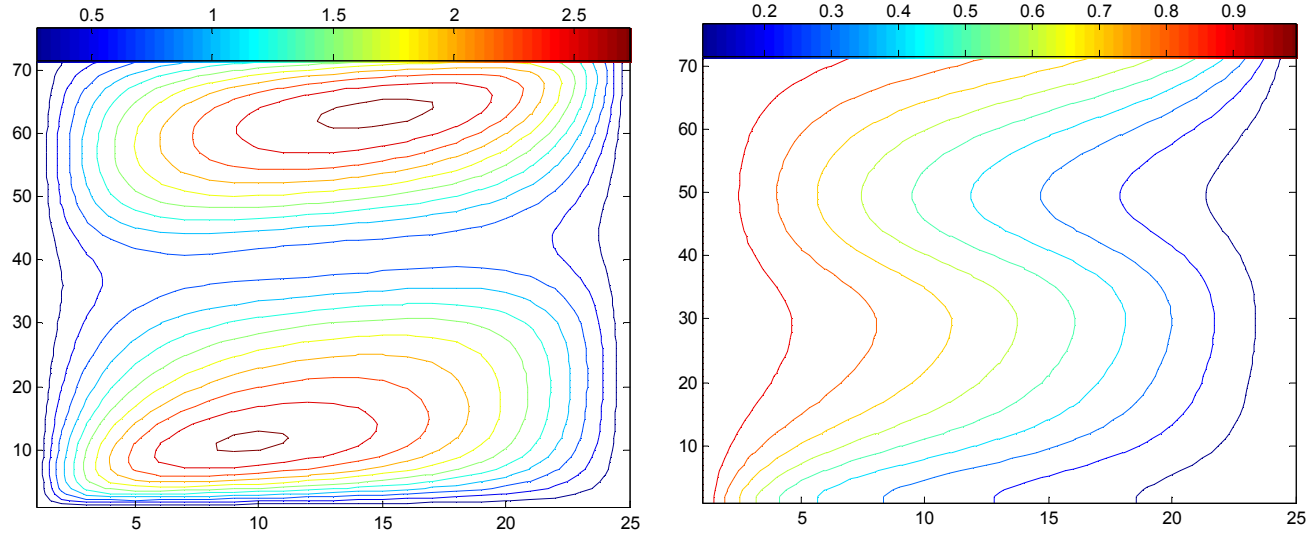

(d)

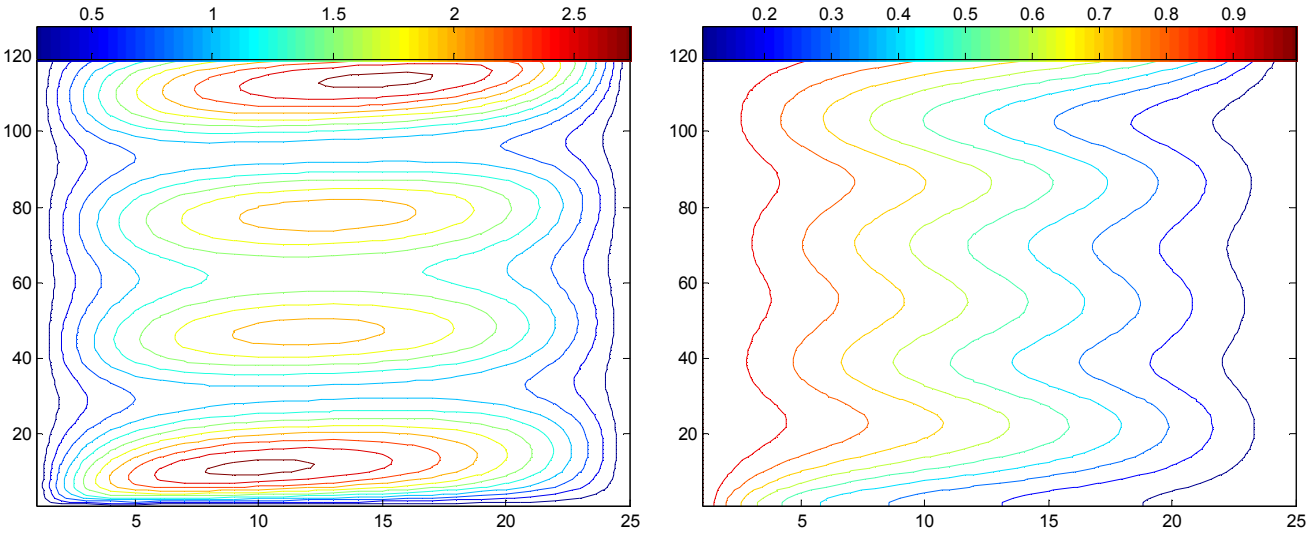

(f)

Fig. 5.8 Typical dimensionless streamline and dimensionless temperature patterns for various aspect ratio of the enclosure (a) $A = 0.4$, (b) $A = 0.6$, (c) $A = 1$, (d) $A = 3$, (f) $A = 5$, for $\emptyset = 30°$, $Ra_w = 100$, $Fr = 0.01$, and $Ha^2 = 0.02$

5.3 The results with viscous and Joule heating effects:

5.3.1 Magneto hydrodynamic effects:

The Magneto hydrodynamic effects can be studied by using different values of the magnetic influence number (Ha^2) in the momentum equation through the magnetic effect term and in the energy equation through the Joule heating effect term. for ∅=30°, A = 1, Fr = 0.01, Ge=0.05. Figure (5.9) shows the relation between the variations of mean Nusselt number at the cold-hand side wall with magnetic influence number. It can be seen that the mean Nusselt number is decreased by increasing the magnetic influence number; due to decreasing in the dimensionless temperature value in the lower half region along the right-hand side wall. Figure (5.10) illustrates the effect of magnetic influence number on the dimensionless streamlines and isotherms patterns, as it is shown, the hot fluid rises up along the left-hand side hot wall and the cold fluid descends along the right-hand side cold wall as seen in fluid isothermal contours. On the other hand, the cold fluid near the right-hand side wall is at lower temperature, and the hot fluid near the left-hand side wall is at higher temperature. By increasing the magnetic influence number the dimensionless temperature value is decreased therefore, the mean Nusselt number and the fluid flow are decreased. At $Ha^2 = 0$ the dimensionless temperature value is increased for the hot fluid in the upper left-hand corner of the enclosure to become larger than 0.9 as well as the dimensionless stream lines are moved to the upper right-hand corner; due to the Gebhart number effects in Joule term. From $Ha^2 = 0.03 - 0.1$ the hot fluid along the left-hand side wall ascends upward and the cold fluid along the right-hand side wall descends downward with smaller dimensionless stream function by comparison with fluid flow at $Ha^2 = 0$, so the heat transfer and fluid flow are decreased. By increasing Ha^2 to reach 1, the magnetic force becomes larger

and the dimensionless stream function of the hot fluid along the left-hand side wall has bigger value than the cold fluid along the right-hand side wall. On the other hand, the fluid in the middle half of the enclosure has two circulations of flow with bigger dimensionless stream function value by comparison with the flow along the walls. At $Ha^2 = 3$ The hot fluid along the left-hand side wall has circulation of flow with bigger dimensionless stream value by comparison with the cold fluid along the opposite wall and in the middle half of the enclosure. So, by increasing Ha^2 the circulation of flow becomes along the left-hand side wall and the dimensionless stream function is decreased to reach negligible value at $Ha^2 = 4$.

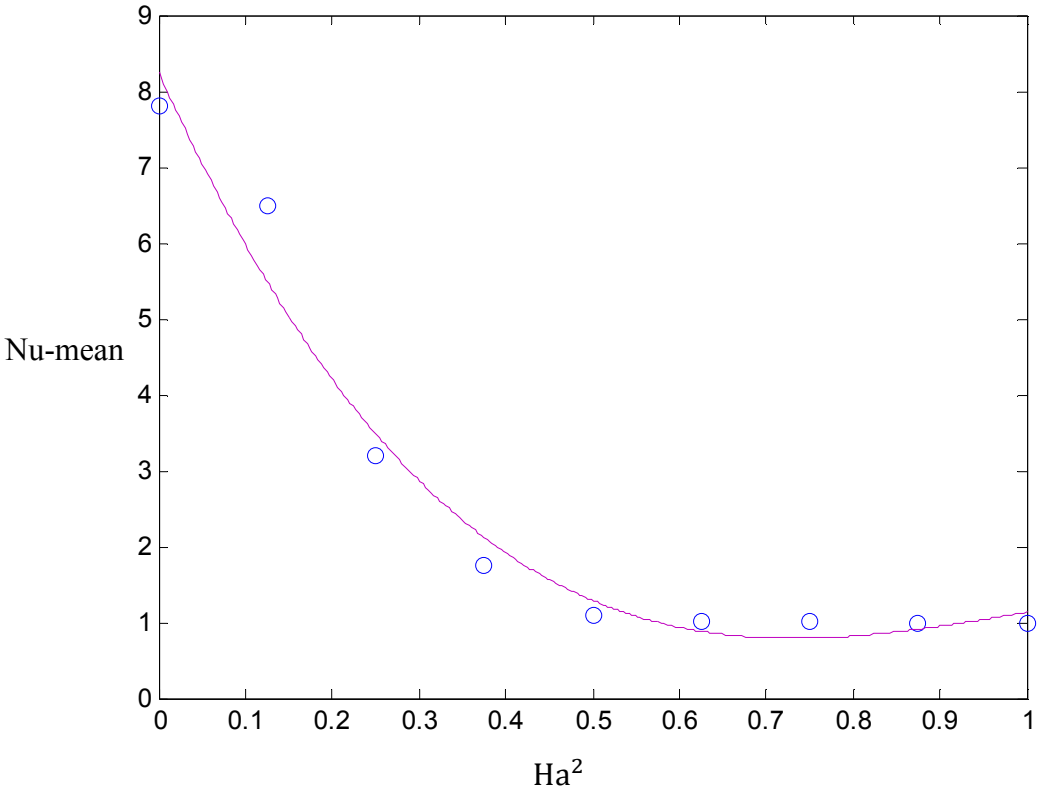

Fig. 5.9 Variation of Nu-mean at the cold-side wall with Ha^2 for an enclosure for Ø=30°, A = 1, Fr = 0.01, Ge = 0.05 and Ra_w = 100

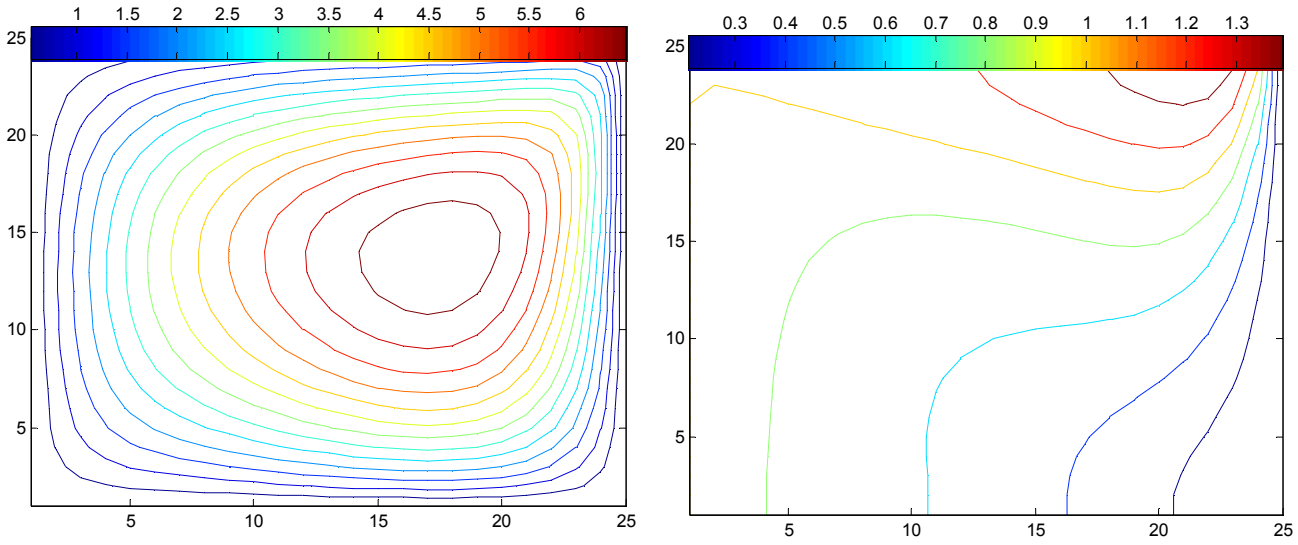

(a)

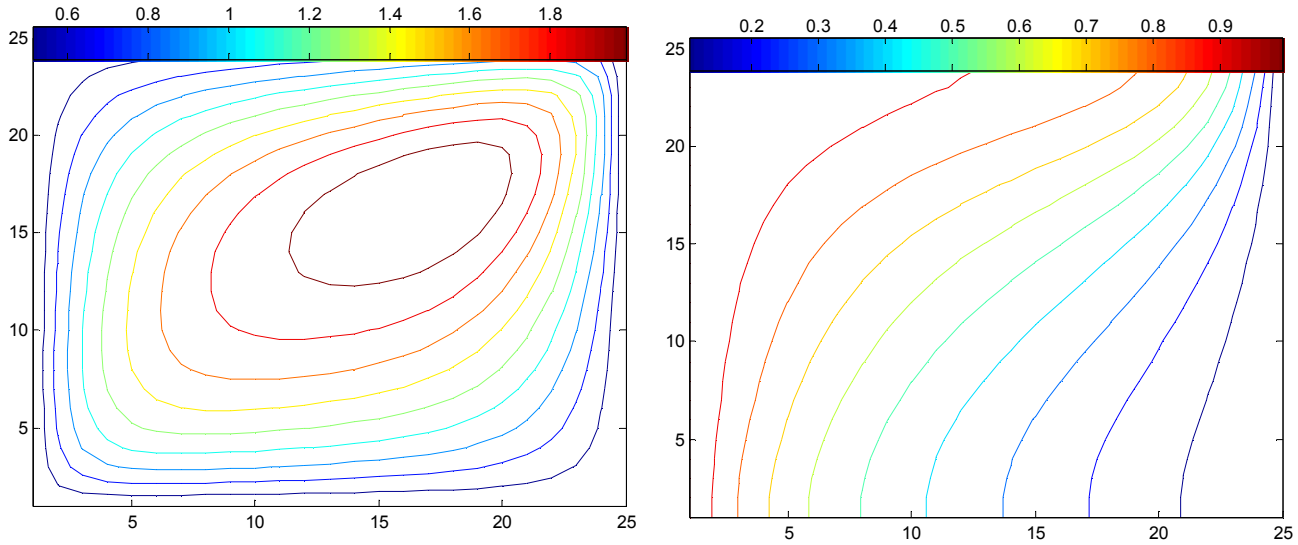

(b)

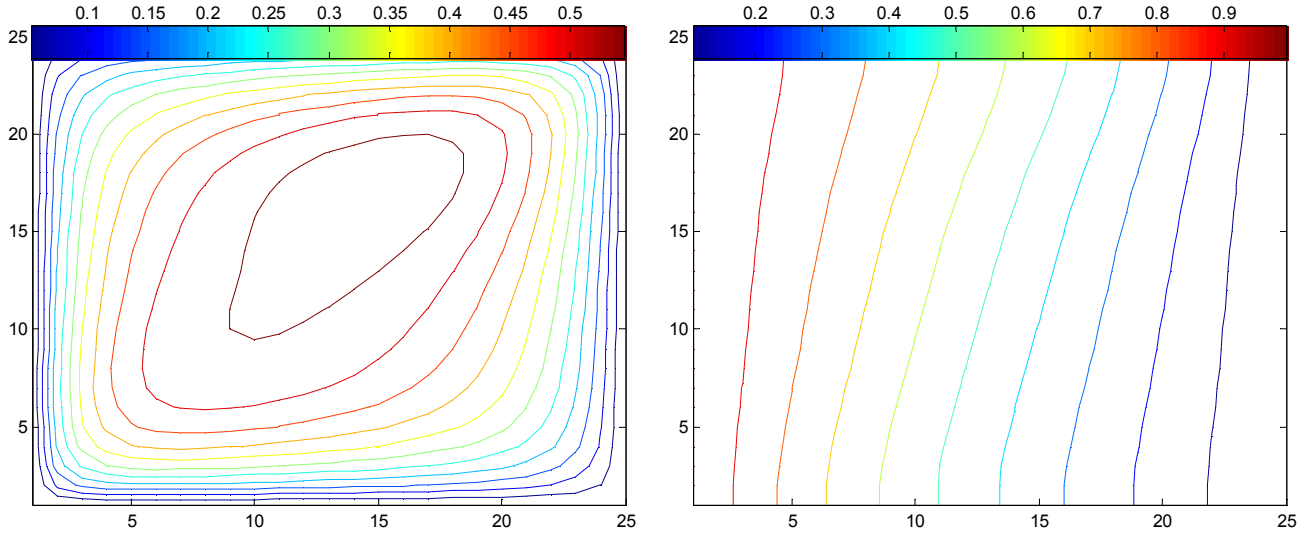

(c)

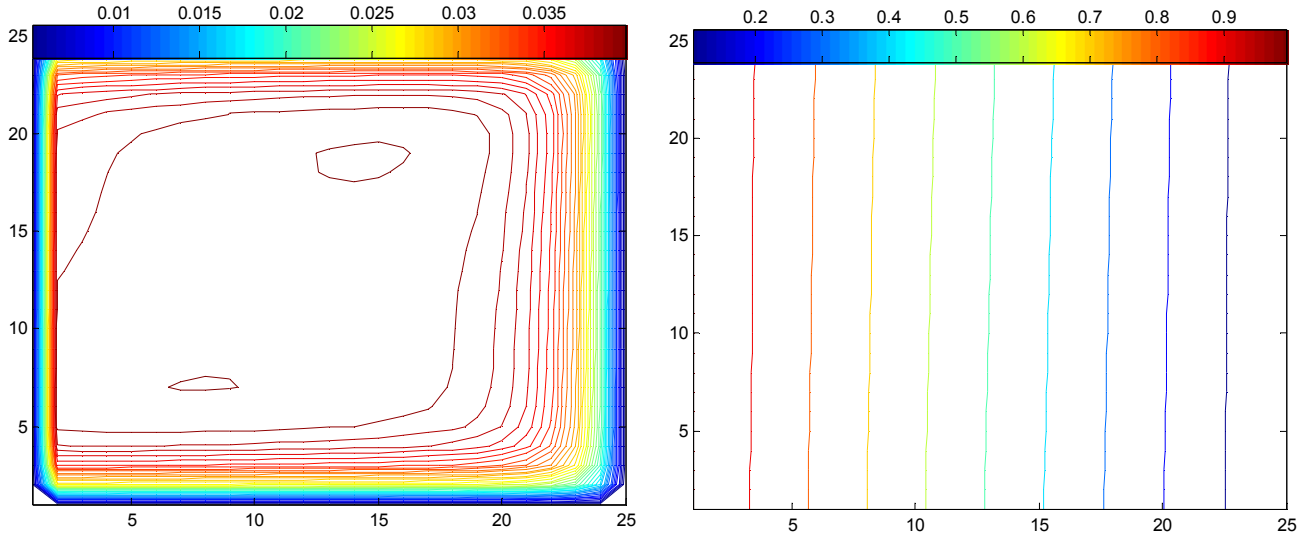

(d)

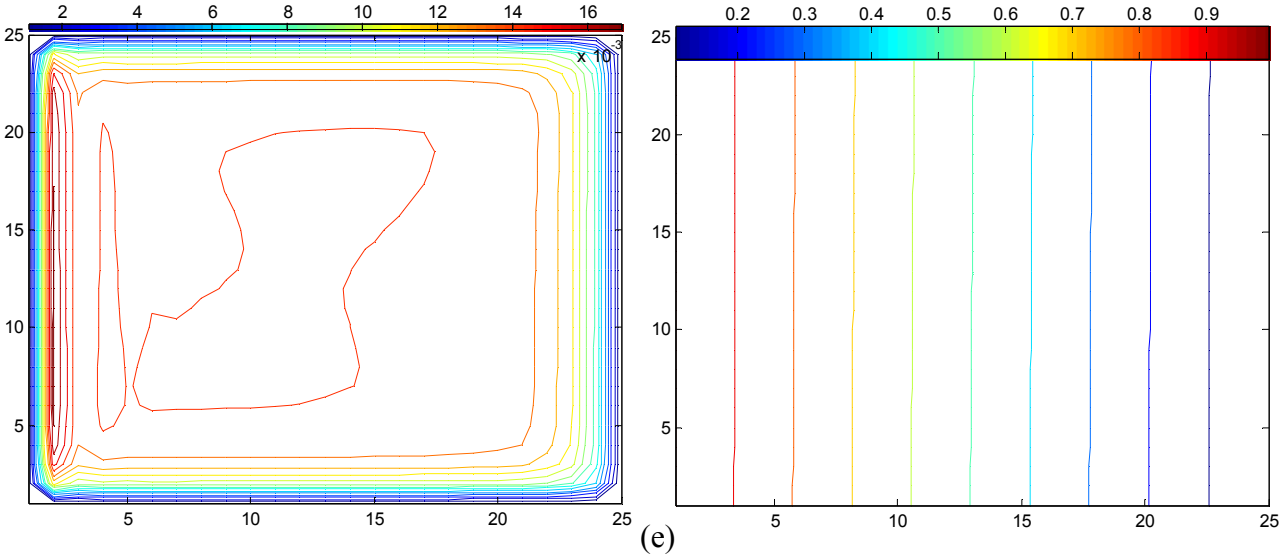

(e)

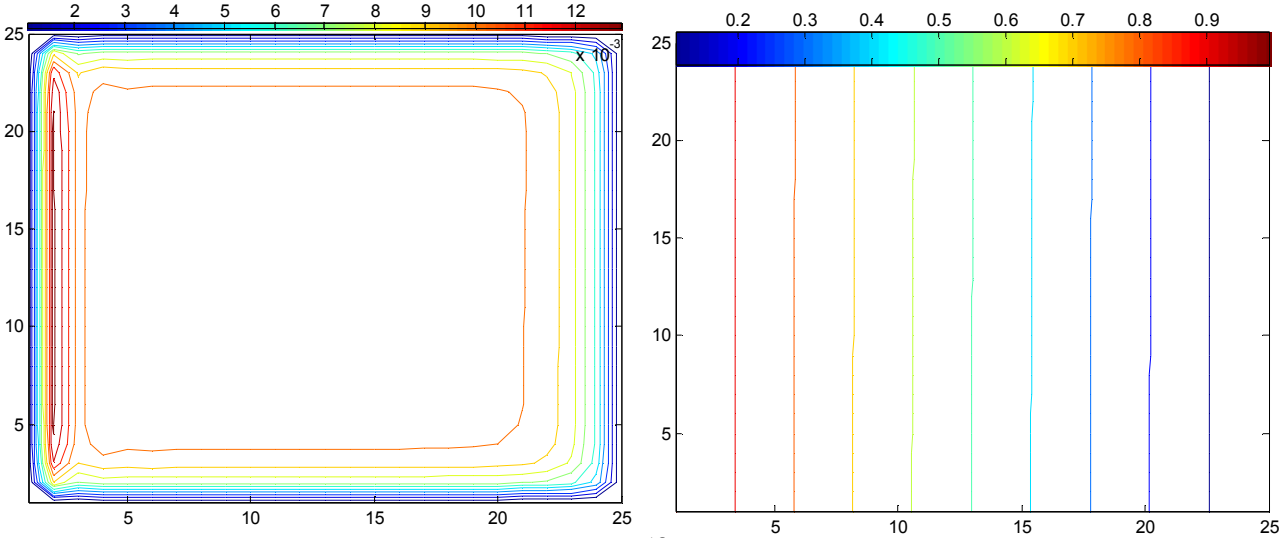

(f)

Fig. 5.10 Typical dimensionless streamline and dimensionless temperature patterns for various magnetic influence number (a) $Ha^2 = 0$, (b) $Ha^2 = 0.03$, (c) $Ha^2 = 0.1$, (d) $Ha^2 = 1$, (e) $Ha^2 = 3$, (f) $Ha^2 = 4$ for Ø=30°, A = 1, Fr = 0.01, Ge = 0.05 and Ra_w = 100

5.3.2 The Gebhart number effects:

Figures (5.11) illustrates the effect of Gebhart number through the viscous and Joule heating terms in the energy equation on the dimensionless streamlines and isotherms patterns with other parameters unchanged, as it is shown, Gebhart number has a certain effect on the heat transfer and fluid flow. By increasing the Gebhart number the dimensionless temperature value is increased therefore, the fluid flow is increased and moved to the upper right-hand corner; this is due to the increasing in hot fluid inside the enclosure and this hot fluid will be moved to the upper left-hand corner and make circulation of fluid. At Ge = 0 the hot fluid rises up along the left-hand side hot wall and the cold fluid descends along the right-hand side cold wall as seen in fluid isothermal contours. On the other hand, the fluid is rotating around the centre of the enclosure with maximum fluid flow by comparison with the flow along the walls. From Ge = 0.02-0.05 the dimensionless temperature of the hot fluid in the upper left-hand corner of the enclosure is increased and the cold fluid in the lower right-hand corner of the enclosure is decreased, therefore, the mean Nusselt number at the cold-hand side wall is decreased. By increasing Ge the dimensionless stream lines are moved to the upper right-hand corner and the dimensionless temperature value is increased for the hot fluid in the upper left-hand corner of the enclosure to become larger than 0.9 at Ge = 0.08; this is due to the increasing in the work done by magnetic field force on the fluid and the increasing in the friction between the fluid layers inside the enclosure. Figure (5.12) shows the relation between the variations of mean Nusselt number at the cold-hand side wall with Gebhart number. It can be seen that the mean Nusselt number is decreased by increasing in the Gebhart number due to increasing in dimensionless temperature in the upper half region along the left-hand side.

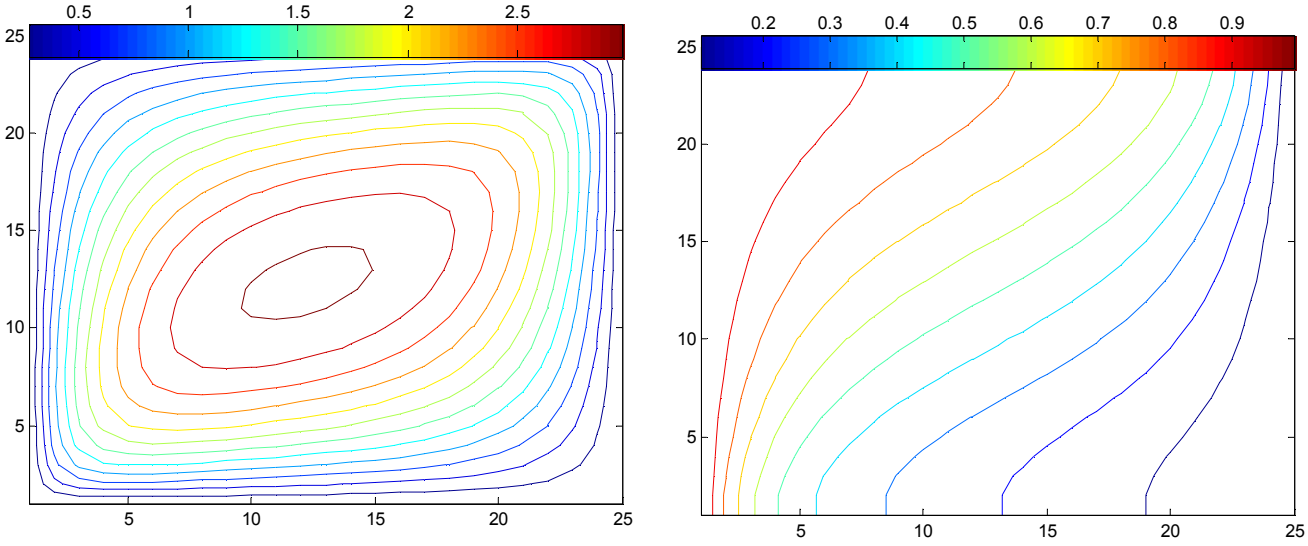

(a)

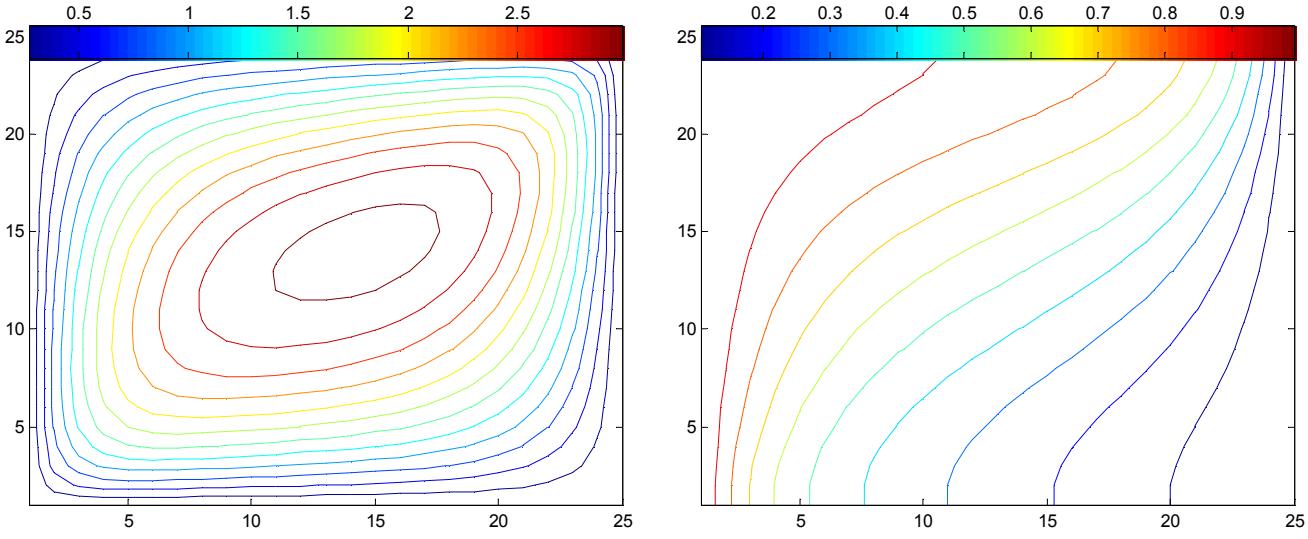

(b)

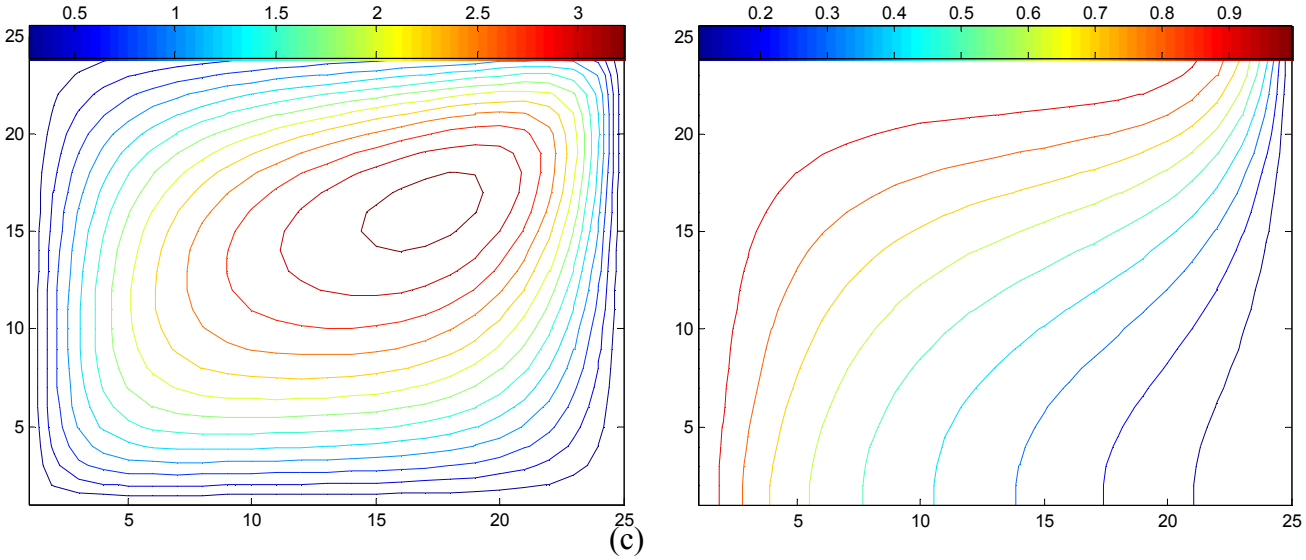

(c)

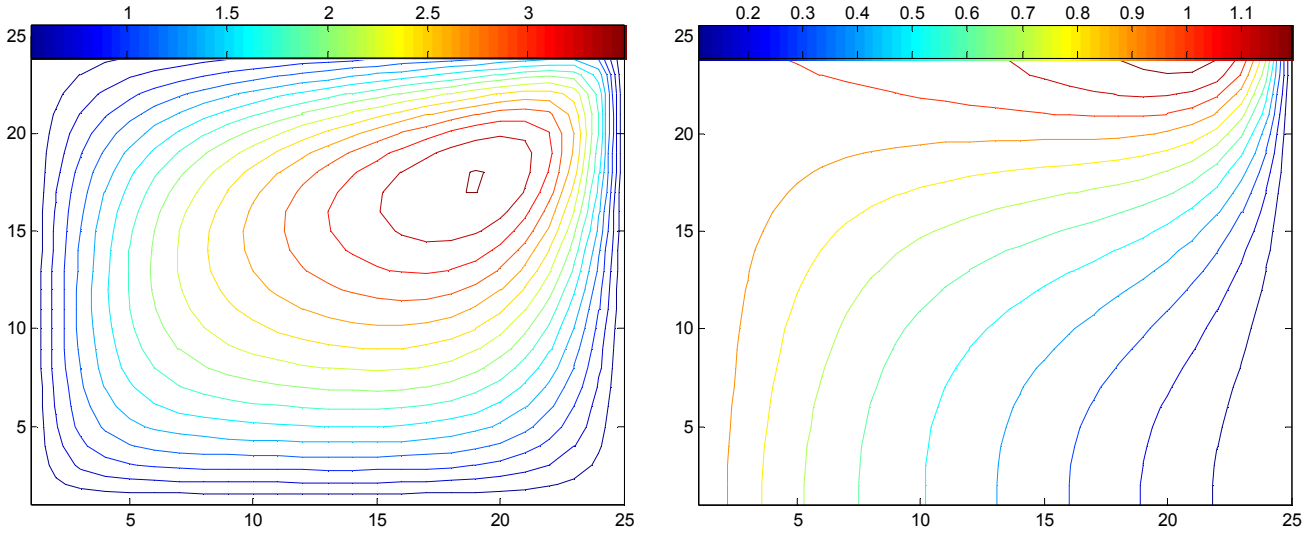

(d)

Fig. 5.11 Typical dimensionless streamline and dimensionless temperature patterns for various Gebhart number (a) $Ge = 0$, (b) $Ge = 0.02$, (c) $Ge = 0.05$, (d) $Ge = 0.08$ for $\emptyset$=30°, $Ha^2 = 0.02$, A = 1, Fr = 0.01, and $Ra_w = 100$

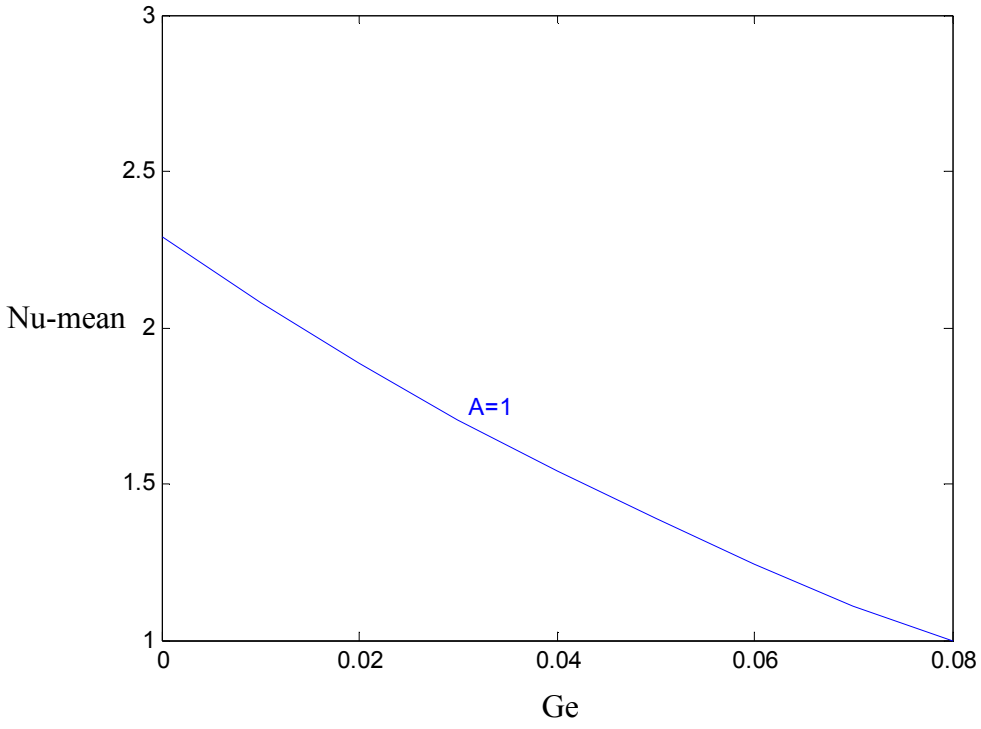

Fig. 5.12 Variation of Nu-mean at the cold-side wall with Ge for an enclosure for Ø=30°,$Ha^2 = 0.02$, A = 1, Fr = 0.01, and Ra_w = 100

5.3.3 Modified Rayleigh number effects:

Figures (5.13) illustrates the effect of Rayleigh number in the momentum equation on the dimensionless streamlines and isotherms patterns with other parameters unchanged, as it is shown, Rayleigh number has a certain effect on the heat transfer and fluid flow. When the Rayleigh number is small, the magnitude of magnetic force has little effect on the heat transfer rate. At $Ra_w = 1$ the hot fluid along the left-hand side wall and the cold fluid along the right-hand side wall have small value of dimensionless stream function of fluid flow, which is 0.015 at the centre of the enclosure. By increasing Ra_w to reach the maximum value which is 100, the magnetic force has larger effect on the heat transfer rate and the value of dimensionless stream line reaches to become 3 at $Ha^2 = 0.02$ at the centre of the enclosure. The values of the mean Nusselt number are shown in Fig. (5.14). It is found that, When the Rayleigh number is small, the value of mean Nusselt number is 1 and then increases to reach the maximum value at $Ra_w = 100$. It can be seen that the variation of Nu-mean with Ra_w for an enclosure for various A, as it is shown, the maximum value of mean Nusselt number is at A=1, this is due to negligible convection heat transfer effects when $Ra_w \to 0$ and the value of Nu-mean = 1 means a pure conduction heat transfer problem.

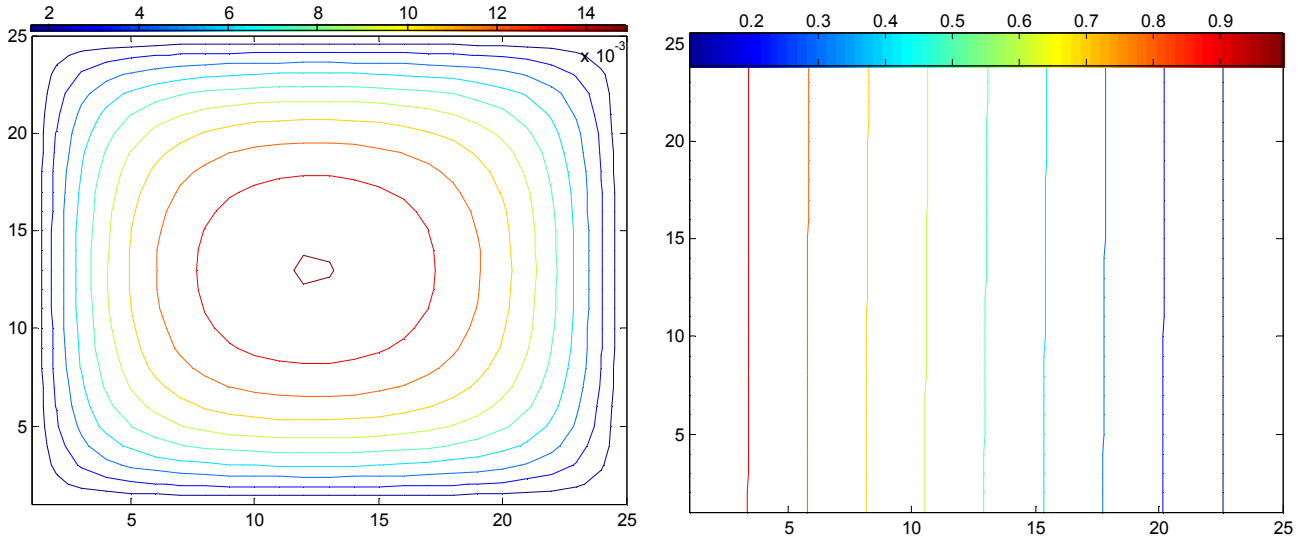

(a)

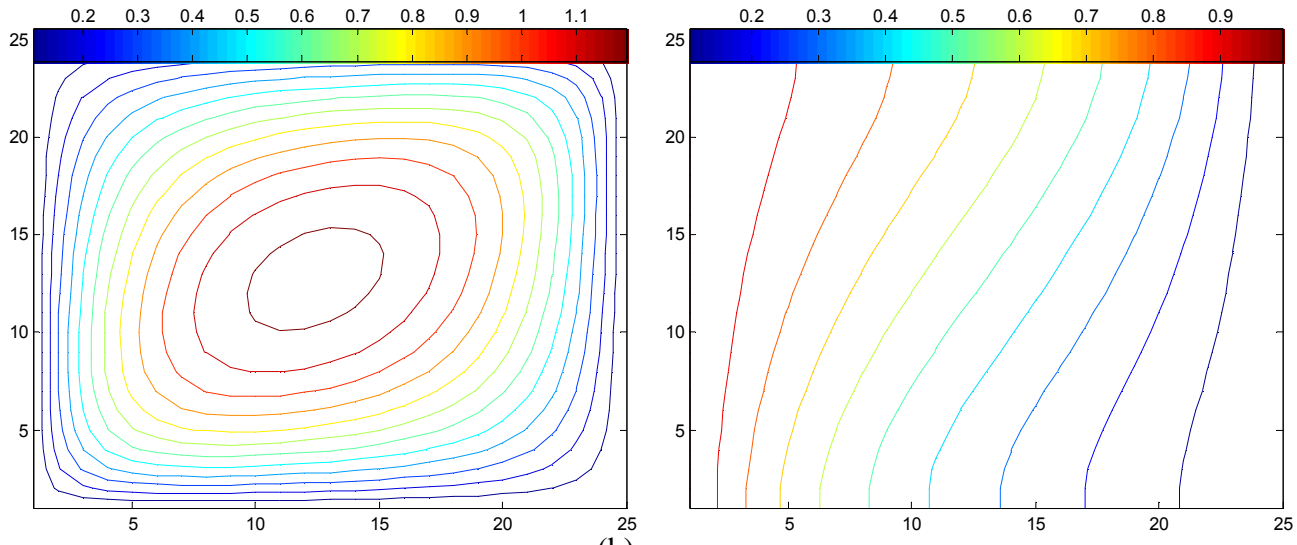

(b)

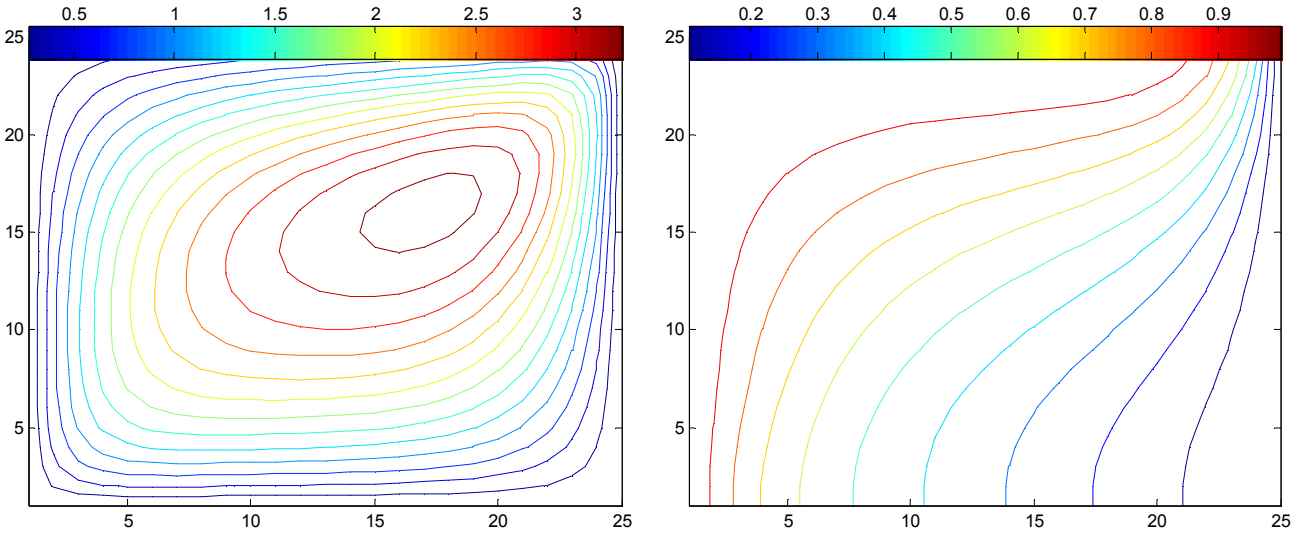

(c)

Fig. 5.13 Typical dimensionless streamline and dimensionless temperature patterns for various Darcy-modified Rayleigh number (a) $Ra_w = 1$, (b) $Ra_w = 50$, (c) $Ra_w = 100$, for Ø=30°, A = 1, Fr = 0.01, Ge=0.05, and $Ha^2 = 0.02$

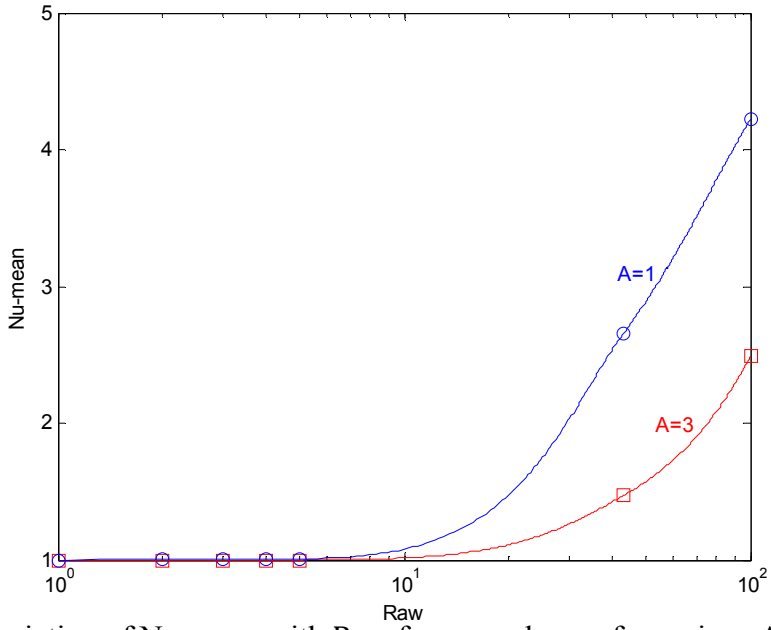

Fig. 5.14 Variation of Nu-mean with Ra_w for an enclosure for various A for Ø=30°, A = 1, Fr = 0.01, Ge=0.05, and $Ha^2 = 0.02$

5.3.4 The inclination angle of the enclosure effects:

In order to examine the effects of inclination angle, computations are carried out for a fluid with the inclined angle varying from 0 to 180°, while other geometric parameters remained unchanged. Numerical results are obtained for (Ra_w = 100, A = 1, Ha^2 = 0.02, Ge=0.05, and Fr = 0.01). Figure (5.15) illustrates the effect of the inclination angle of the enclosure on the dimensionless streamlines and isotherms patterns with other parameters unchanged, as it is shown, $\emptyset$ has a certain effect on the heat transfer and fluid flow. When $\emptyset = 0$ the hotter fluid along the left-hand side wall descends downward and the colder fluid along the right-hand side wall ascends upward due to the usual gravitational buoyancy force, which forms a counterclockwise flow. At $\emptyset = 30°$ the hot fluid along the left-hand side wall ascends upward and the cold fluid along the right-hand side wall descends downward which forms a clockwise flow as well as $\emptyset = 90°$. At $\emptyset = 30°$ the fluid flow have the largest dimensionless streamline function by comparison with the flow at differentiating value of $\emptyset$. At $\emptyset$ =180° the magnitude of magnetic force has not effect on the heat transfer rate. The hot fluid along the left-hand side wall and the cold fluid along the right-hand side wall have not flow when $\emptyset$ =180°.

Figure (5.16, 5.17, and 5.18) show the relation between the variation of mean Nusselt number and dimensionless center-stream function with angle of inclination for an enclosure for various Ha^2, Ra_w, and Ge, respectively. It can be seen that at $\emptyset = 30°$ mean Nusselt number and dimensionless center-stream function have maximum values. On the other hand, it can be seen that the dimensionless center-stream function is decreased by increasing in the magnetic influence number and it is increased by increasing the modified Rayleigh number; this is due retardation effect of the magnetic field and favorable effect of the buoyancy forces.

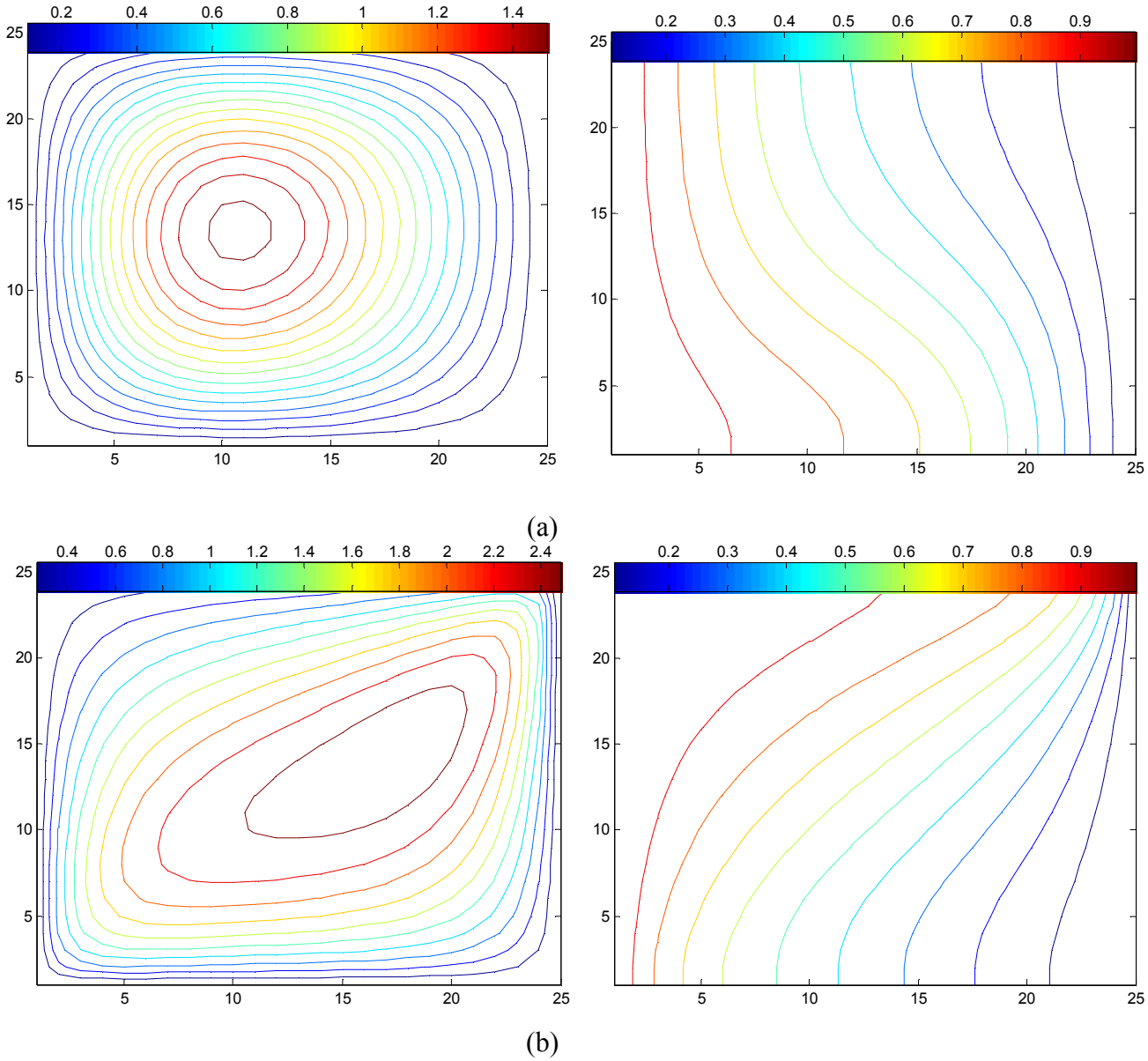

Fig. 5.15 Typical dimensionless streamline and dimensionless temperature patterns for various inclination angle of the enclosure (a) $\emptyset = 0$, (b) $\emptyset = 90°$ for $Ra_w = 100$, A = 1, Fr = 0.01, Ge=0.05, and $Ha^2 = 0.02$

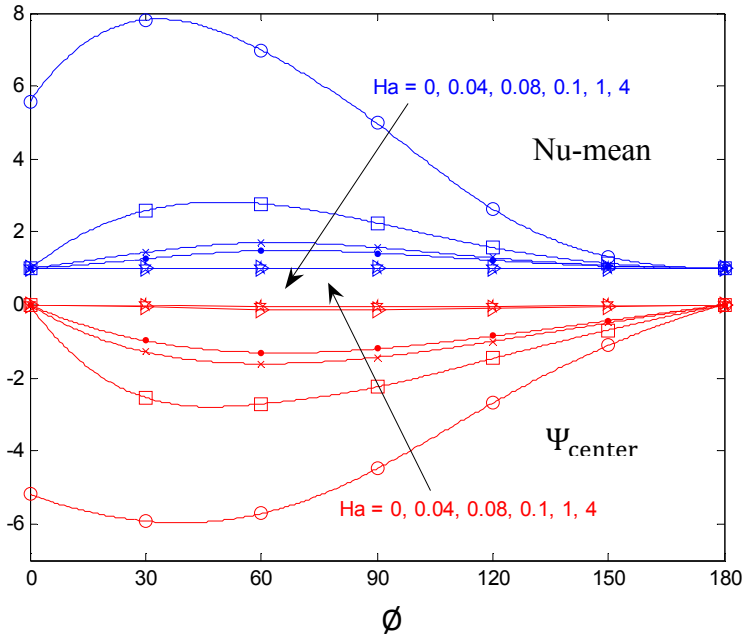

Fig. 5.16 Variation of mean Nusselt number and dimensionless center-stream function with angle of inclination for an enclosure for various Ha^2 for $Ra_w = 100$, A = 1, Fr = 0.01, and Ge=0.05

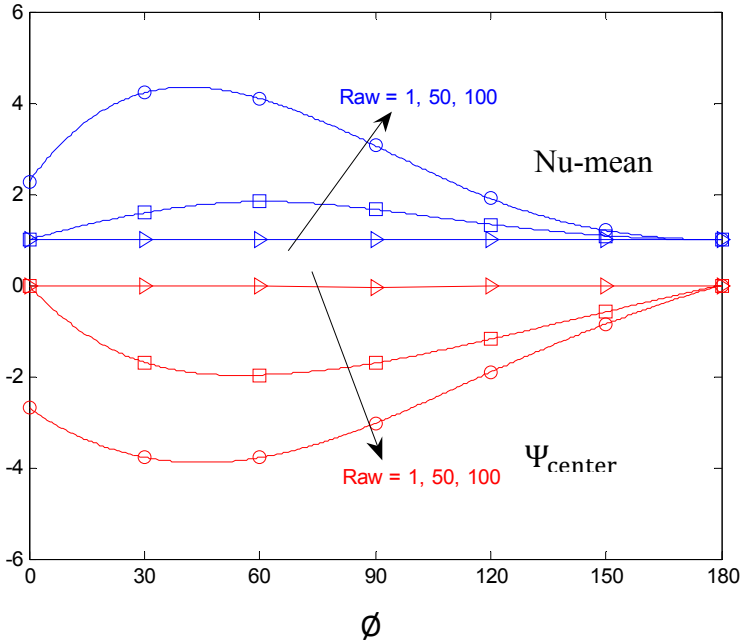

Fig. 5.17 Variation of mean Nusselt number and dimensionless center-stream function with angle of inclination for an enclosure for various Ra_w for A = 1, Fr = 0.01, Ge=0.05, and $Ha^2 = 0.02$

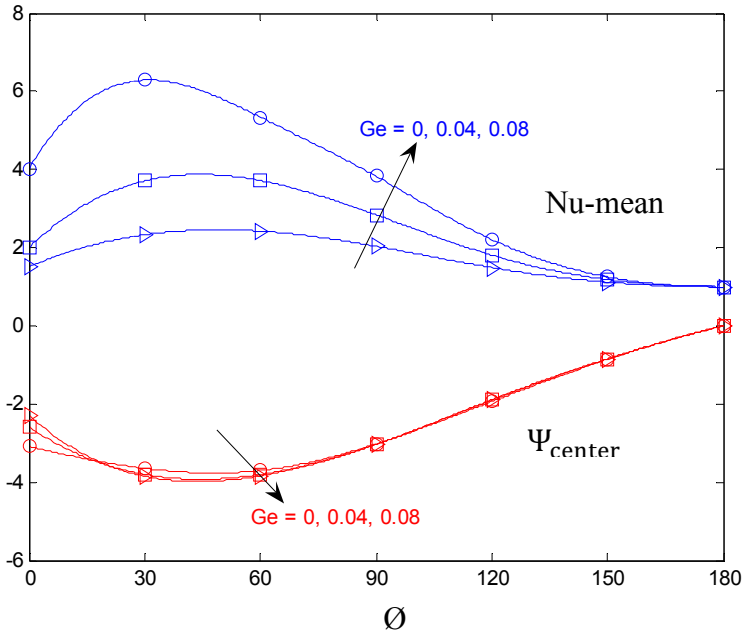

Fig. 5.18 Variation of mean Nusselt number and dimensionless center-stream function with angle of inclination for an enclosure for various Ge for A = 1, Fr = 0.01, Ra_w = 100, and $Ha^2 = 0.02$

5.3.5 The aspect ratio of the enclosure effects:

Figure (5.19) illustrates the effect of aspect ratio of the enclosure on the dimensionless streamlines with other parameters unchanged, as it is shown, it is found that, When A=1 the fluid is rotating around the centre of the enclosure so, it have one circulation of flow. At A=3 the fluid has two circulations of flow, respectively. The values of the mean Nusselt number are shown in Figure (5.14). It can be seen that the variation of Nu-mean with Ra_w for an enclosure for various A, as it is shown, the heat transfer is decreased with the increasing of aspect ratio when the aspect ratio bigger than 1.

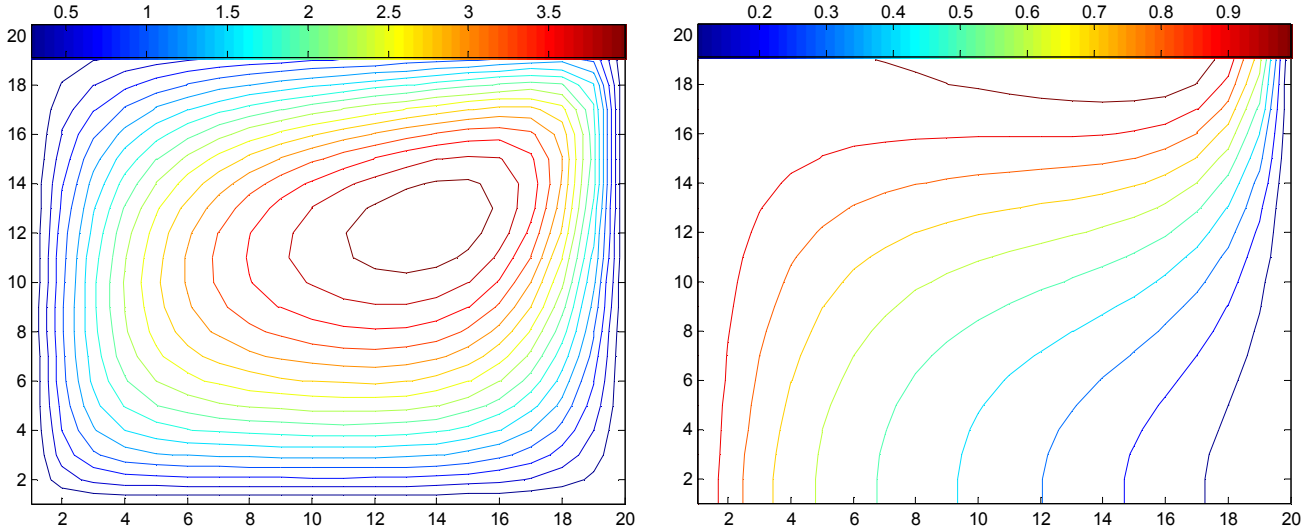

(a)

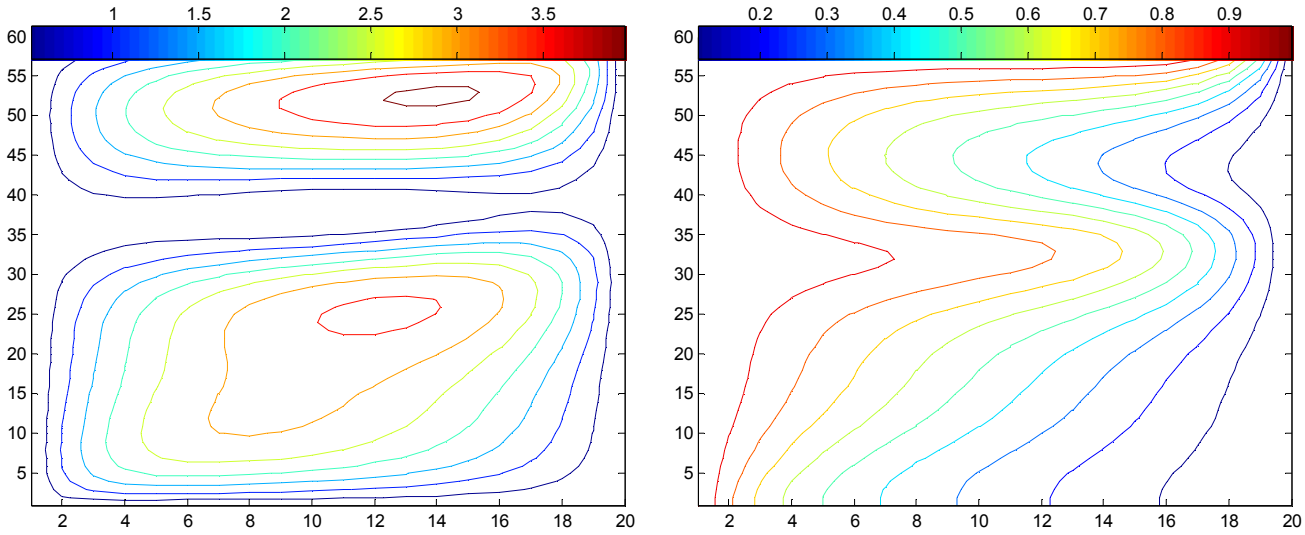

(b)

Fig. 5.19 Typical dimensionless streamline and dimensionless temperature patterns for various aspect ratio of the enclosure (a) $A = 1$, (b) $A = 3$, for $\emptyset = 30°$, $Ra_w = 100$, $Fr = 0.01$, $Ge = 0.05$ and $Ha^2 = 0.02$

5.4 Forchheimer number effects:

Figures (5.20) illustrates the effect of Forchheimer number in the momentum equation on the dimensionless streamlines and isotherms patterns with other parameters unchanged, as it is shown, Fr has a certain effect on the heat transfer and fluid flow by increasing the Forchheimer number the circulation of flow becomes in the upper portion of the enclosure and the dimension less stream function values are decreased; this is due to the increasing in the porosity inside the enclosure. On the other hand, the heat transfer inside the enclosure becomes by conduction; due to decreasing in Nusselt number. Figure (5.21) shows the relation between the variations of mean Nusselt number with Forchheimer number. It can be seen that the mean Nusselt number is decreased by increasing the Forchheimer number; this is due to decreasing in dimensionless temperature in the upper half region along the left-hand side and the lower half region along the right-hand side wall.

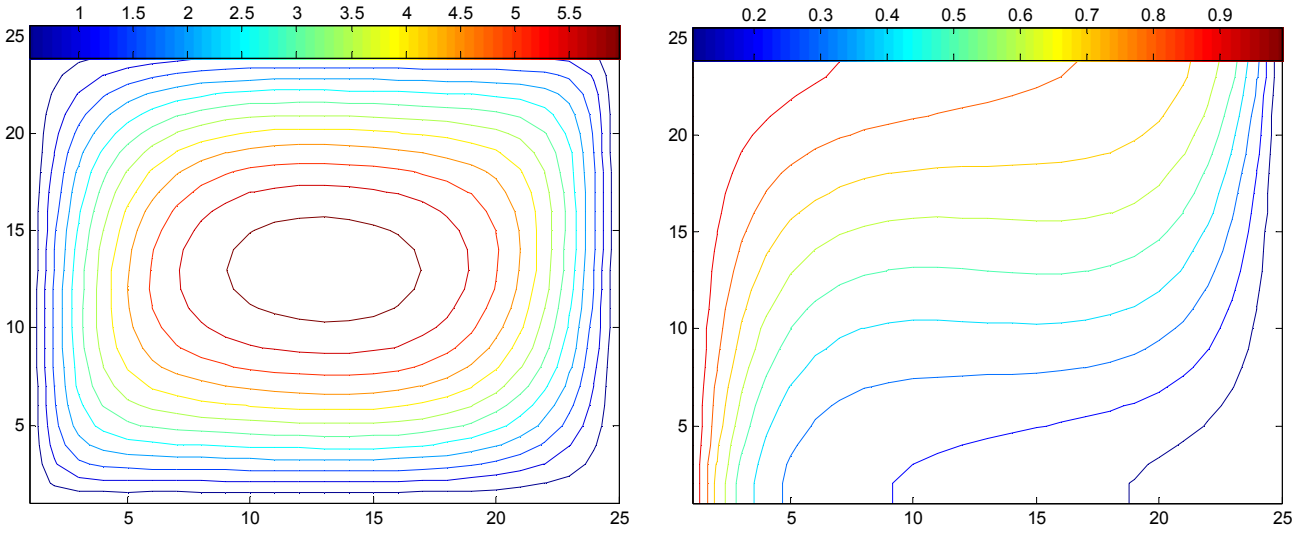

(a)

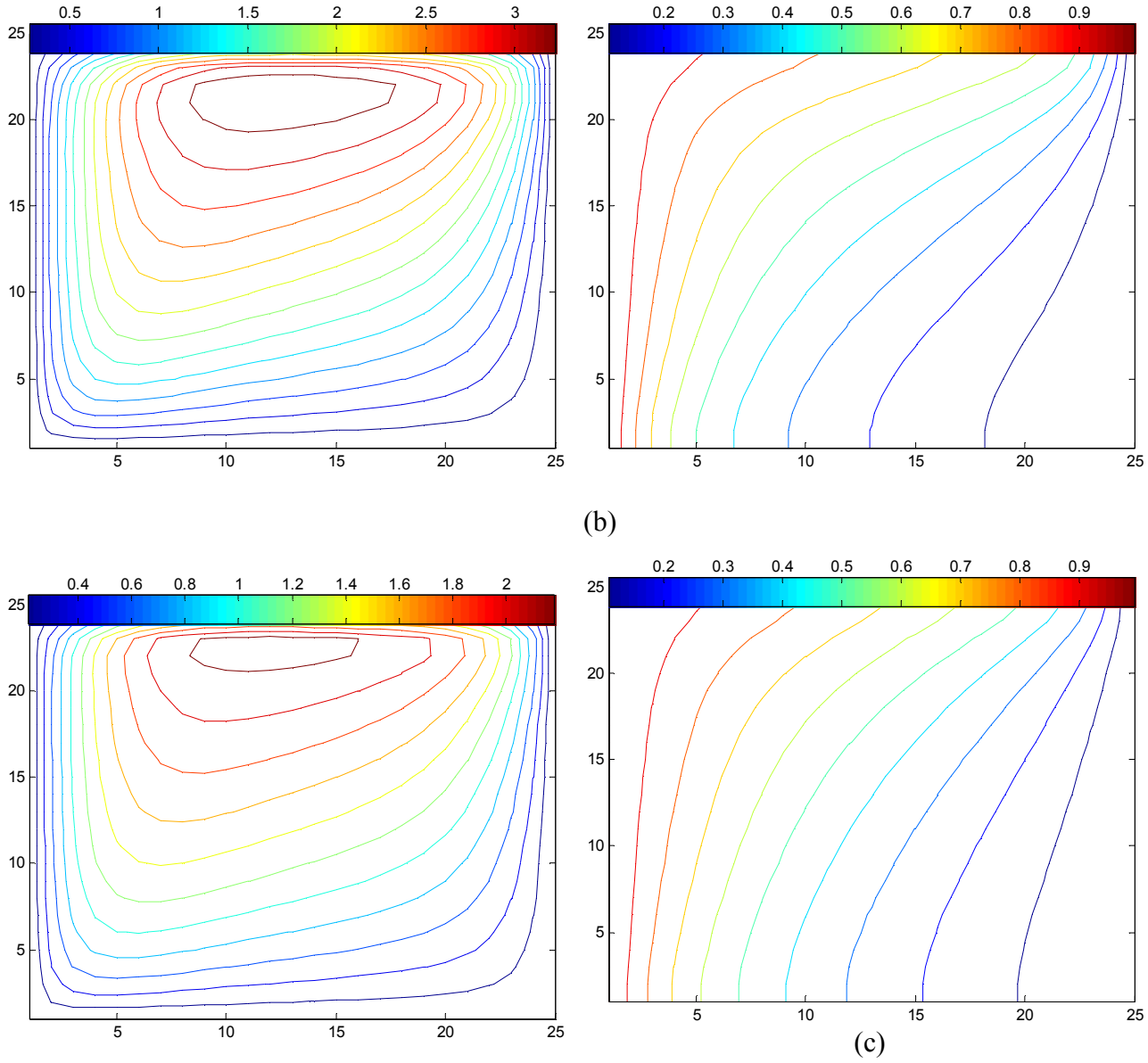

Fig. 5.20 Typical dimensionless streamline and dimensionless temperature patterns for various Forchheimer number (a) $Fr = 0$, (b) $Fr = 0.008$, (c) $Fr = 0.02$, for Ø=30°, A = 1, $Ha^2 = 0$, Ge=0, and $Ra_w = 100$

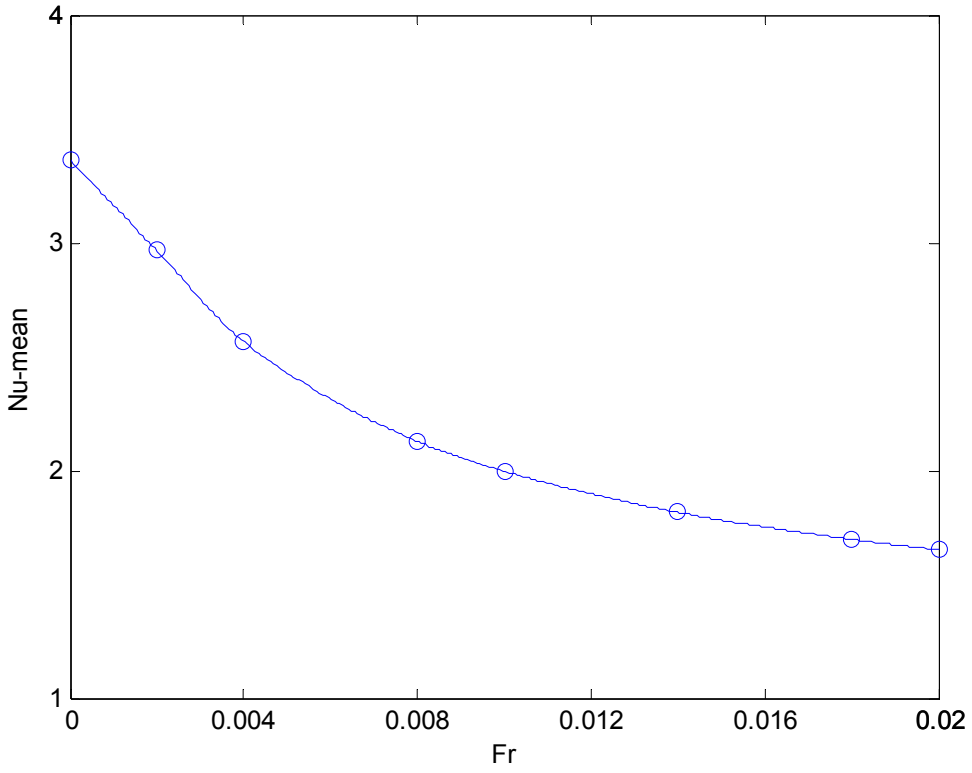

Fig. 5.21 Variation of Nu-mean with Forchheimer number for an enclosure for Ø=30°, A = 1, $Ha^2 = 0$, Ge=0, and Ra_w = 100

Chapter 6

Conclusion and Recommendation

6.1 Conclusion:

Flow field and heat transfer characteristics have been analyzed numerically for the magnetohydrodynamics natural convection heat transfer problem inside a porous media filled inclined rectangular enclosures. Finite difference scheme method was used. Based on the previous results the following may be concluded:

(1) Heat transfer and fluid flow are decreased with the increasing of magnetic influence number.

(2) When the Darcy number is small, the magnitude of magnetic force has little effect on the heat transfer rate. Heat transfer and fluid flow are increased with the increasing of Darcy-modified Rayleigh number.

(3) Inclination angle has a certain effect on the heat transfer and fluid flow.

(4) Aspect ratio also affects the heat transfer and fluid flow. Heat transfer is decreased with the increasing of aspect ratio.

(5) By increasing Ge heat transfer for the hot fluid in the upper left-hand corner of the enclosure and fluid flow are increased.

(6) By increasing Ge the viscous and Joule heating effects are increased and the fluid flow is moved to the upper right-hand corner.

6.2 Recommendations:

In the present work, the MHD-natural convection interaction inside rectangular porous filled enclosures are going to be formulated using continuity, Forchheimar of Darcy law and energy, the governing equations are going to be transformed into dimensionless form using a set of suitable variables than solved using a finite difference scheme. The following suggestions for further investigation based on the previous work are recommended:

1. Studying the effect of changing the boundary condition.
2. Studying the problem with variations of both velocity and temperature fields in time.
3. Studying the problem with add another term to the governing equations, such as the analogous to the Laplacian term that appears in the Navier-Stokes equation.

REFERENCES:

Al-Zubi, Morad and H. M. Duwairi. (2007). **MHD Convection over non Isothermal Ellipse Embedded in Fluid Saturated Porous Medium**, Int. J. Heat and Technology, in press, vol. 25.

Aldoss, T. K., AI-Namir, M. A., Jarrah, M. A., and AI-Sha'er, B. J. (1995), **Magnetohydrodynamic mixed convection from a vertical plate embedded in a porous medium**, Numerical Heat Transfer, part A, vol. 28, pp. 635-645.

Boussinesq, J. (1903). **Th´eorie Analytique de la Chaleur, Gauthier-Villars, Paris**. vol. 2.

Chandra, B. and Gosh, N. (2001), **MHD flow of a visco-elastic liquid through porous - medium**, International Journal of Numerical Methods for Heat and Fluid, vol. 11, pp. 682-698.

Duwairi, H. M. and Damseh, R. A. (2004, a), **Magnetohydrodynamic natural convection heat transfer from radiate vertical porous surfaces**, Heat and Mass Transfer, vol. 40, pp. 787-792.

Duwairi, H. M. and Duwairi, R. M. (2004, b), **Thermal radiation effects on MHD-Rayleigh flow with constant surface heat flux**, Heat Mass Transfer, vol. 41, pp. 51-57.

Duwairi H. M. and Sufian Al-Araj (2004 c), **MHD-Mixed Convection Along Radiant Vertical Cylinder**, Conference of thermal Engineering: Theory and Application, 31/5-4/6, Lebanon.

Duwairi H. M., Rebhi. A. Damseh and Bourhan Tashtoush. (2006), **Transient Non-Boussinesq MHD-Free Convection Flows Over a Vertical Surface**. Int. J. Fluid Mechanics Research, vol. 2, pp.173-152.

Duwairi H. M. and Y. Al-Kablawi. (2006), **MHD-Conjugate Mixed Convection Heat Transfer Over a Vertical Hollow Cylinder Embedded in a Porous Medium**, Int. J. of Heat and Technology, vol. 24, pp. 123-128.

Ergun, S. (1952). **Fluid flow through packed columns**. Chem. Engrg. Prog. 48, 89–94.

Forchheimer, P. (1901), **Wasserbewegung durch Boden**, Zeitschrift des Vereines Deutscher Ingenieure 45, 1736–1741 and 1781–1788.

Garandet, J. P., Alboussiere, T. and Moreau, R. (1992), **Buoyancy driven convection in a rectangular enclosure with a transverse magnetic field**, Int.J. Heat Mass Transfer, vol. 35, pp. 741-749.

Hammad, I. M. and H. M. Duwairi (2008), **Mixed Convection Heat Transfer for a non-Newtonian Fluid around a Cylinder or Sphere Embedded in Porous Media**, Int. J. Heat and Technology, in press.

Henoch, C. W. and Meng, J. C. S. (1991), **Magnetohydrodynamic turbulent boundary layer control using external direct current crossed surface poles**, ASME, vol. 5(3), pp.115-121.

Hossain, M. A. (l992), **Viscous and Joule heating effects on MHD-free convection flow with variable plate temperature**, Int. J. Heat Mass Transfer, vol. 35, pp. 3485-3487.

Holman, J. A. (1990). **Heat Transfer, Ch12**. Newyork: McGraw-Hill Co.

Jha, B. K. (2001), **Natural convection in unsteady MHD Couette flow**, Heat and Mass Transfer, vol. 37, pp. 329-331.

Joseph, D. D. (1976). **Stability of Fluid Motions II**, Springer, Berlin.

Joseph, D. D., Nield, D. A. and Papanicolaou, G. (1982), **Nonlinear equation governing flow in a saturated porous medium**, Water Resources Res. 18, pp. 1049–1052 and 19, 59.

Kim, S. and Lee, C. (2000), **Numerical investigation of cross flow around a circular cylinder at a low-Reynolds number flow under an electromagnetic force**, Experiments in Fluids, vol. 28, pp. 252-260.

Lage, J. L. (1998), **The fundamental theory of flow through permeable media: from Darcy, (to turbulence. Transport Phenomena in Porous Media** (eds. D.B. Ingham and I. Pop Elsevier, Oxford, pp.1–30.

Nield, P. A. and Bejan, A. (1999), **Convection in Porous Media, (2nd ed.)**, New York:Springer-verlag.

Oberbeck,A.(1879). **Ueber die W¨armeleitung der Fl¨ussigkeiten bei Ber¨ucksichtigung der Str¨omungen infolge von Temperaturdifferenzen**. *Ann. Phys. Chem*. **7**, 271–292.

Oosthuizen, P.H. and D.Naylor (1973), **An Introduction to convective heat transfer analysis**, McGraw-Hill, New York, NY.

Raptis, A. and Singh, A. K. (1983), **MHD free convection flow past an accelerated vertical plate**, Int. Comm. Heat Mass Transfer, vol. 10, pp.313-321.

Sparrow, E. M. and Cess, R. D. (1961), **Effect of magnetic field on free convection heat transfer**, Int. J. Heat Mass Transfer, vol. 3, pp.267-273.

الحمل الحراري الطبيعي الكهرومغناطيسي في وسط مسامي يملأ جسم محصور

إعداد

فادي غسان علي شحاده

المشرف

الدكتور حمزة الدويري

ملخص

في هذا العمل الحمل الحراري الطبيعي الكهرومغناطيسي في وسط مسامي يملأ جسم محصور مستطيل الشكل ومائل بزاوية بظهور تأثير كل من الحرارة الناتجة من الجول واللزوجة سيتم البحث عنها numerically. حدود الجسم المحصور وضعت بحيث يكون جدارين adiabatic و الآخرين isothermal. معادلات العزم والطاقة سيتم تحويلها إلى dimensionless form باستخدام متغيرات معينة وبعد ذلك سيتم حلها باستخدام finite difference scheme. The governing parameters هي تأثير الحمل المغناطيسي و تأثير رقم جيبهارت و تأثير Rayleigh numberوتأثير الزاوية وتأثير نسبة الطول للعرض للجسم المحصور. النتائج التي تم الحصول عليها بينت نقصان إنتقال الحرارة و جريان المائع بزيادة الحمل المغناطيسي ولقد تبين أنه بزيادة Rayleigh number ونسبة الطول للعرض للجسم المحصور سوف يزداد كل من إنتقال الحرارة و جريان المائع. بزيادة Gebhart number سوف يزداد كل من إنتقال الحرارة و جريان المائع.